



UNIVERSIDADE ESTADUAL DE CAMPINAS  
Instituto de Biologia

GABRIEL BANSTARCK MARANDOLA

EVALUATION OF CO<sub>2</sub> RISING EFFECTS ON UNDERSTORY  
VEGETATION TRANSPIRATION IN CENTRAL AMAZONIA  
THROUGH AN EXPERIMENT-MODELING INTEGRATED  
APPROACH

AVALIAÇÃO DOS EFEITOS DO CO<sub>2</sub> ELEVADO SOBRE A  
TRANSPIRAÇÃO DA VEGETAÇÃO DE SUB-BOSQUE NA  
AMAZÔNIA CENTRAL ATRAVÉS DE INTEGRAÇÃO  
EXPERIMENTO-MODELAGEM

Campinas  
2024

GABRIEL BANSTARCK MARANDOLA

EVALUATION OF CO<sub>2</sub> RISING EFFECTS ON UNDERSTORY VEGETATION  
TRANSPIRATION IN CENTRAL AMAZONIA THROUGH AN  
EXPERIMENT-MODELING INTEGRATED APPROACH

AVALIAÇÃO DOS EFEITOS DO CO<sub>2</sub> ELEVADO SOBRE A TRANSPIRAÇÃO  
DA VEGETAÇÃO DE SUB-BOSQUE NA AMAZÔNIA CENTRAL ATRAVÉS DE  
INTEGRAÇÃO EXPERIMENTO-MODELAGEM

Master Thesis presented to the Institute of  
Biology of the University of Campinas in  
partial fulfillment of the requirements for the  
degree of Master of Sciences in Ecology.

Dissertação de Mestrado apresentada ao  
Instituto de Biologia da Universidade Estadual  
de Campinas como parte dos requisitos para a  
obtenção do título de Mestre em Ecologia.

**Supervisor/Orientador: Prof. Dr. David Montenegro Lapola**

ESTE EXEMPLAR CORRESPONDE À  
VERSÃO FINAL DA DISSERTAÇÃO DE  
MESTRADO DEFENDIDA POR GABRIEL  
BANSTARCK MARANDOLA E ORIENTADA  
PELO PROF. DR. DAVID MONTENEGRO  
LAPOLA.

Campinas  
2024

Ficha catalográfica  
Universidade Estadual de Campinas (UNICAMP)  
Biblioteca do Instituto de Biologia  
Mara Janaina de Oliveira - CRB 8/6972

M325e Marandola, Gabriel Banstarck, 1999-  
Evaluation of CO<sub>2</sub> rising effects on understory vegetation transpiration in  
Central Amazonia through an experiment-modeling integrated approach /  
Gabriel Banstarck Marandola. – Campinas, SP : [s.n.], 2024.

Orientador: David Montenegro Lapola.  
Dissertação (mestrado) – Universidade Estadual de Campinas (UNICAMP),  
Instituto de Biologia.

1. Mudanças climáticas. 2. Água - Aspectos Ambientais - Amazônia. 3.  
Modelos matemáticos. 4. Ecologia Vegetal - Amazônia. I. Lapola, David  
Montenegro, 1982-. II. Universidade Estadual de Campinas (UNICAMP).  
Instituto de Biologia. III. Título.

Informações Complementares

**Título em outro idioma:** Avaliação dos efeitos do CO<sub>2</sub> elevado sobre a transpiração da  
vegetação de sub-bosque na Amazônia Central através de integração experimento-  
modelagem

**Palavras-chave em inglês:**

Climate changes

Water - Environmental Aspects - Amazon River Region

Mathematical models

Plant Ecology - Amazon River Region

**Área de concentração:** Ecologia

**Titulação:** Mestre em Ecologia

**Banca examinadora:**

David Montenegro Lapola [Orientador]

Cleiton Breder Eller

Simone Aparecida Vieira

**Data de defesa:** 29-08-2024

**Programa de Pós-Graduação:** Ecologia

**Identificação e informações acadêmicas do(a) aluno(a)**

- ORCID do autor: <https://orcid.org/0000-0002-7371-7980>

- Currículo Lattes do autor: <http://lattes.cnpq.br/6282536152464963>

Campinas, 24 de outubro de 2024.

## COMISSÃO EXAMINADORA

**Prof. Dr. David Montenegro Lapola**

**Profa. Dra. Simone Aparecida Vieira**

**Prof. Dr. Cleiton Breder Eller**

*Os membros da Comissão Examinadora acima assinaram a Ata de Defesa, que se encontra no processo de vida acadêmica do aluno.*

A Ata de Defesa com as respectivas assinaturas dos membros encontra-se no SIGA/Sistema de Fluxo de Dissertações/Teses e na Secretaria do Programa de Pós-Graduação em Ecologia do Instituto de Biologia.

# Agradecimentos

Conduzir e chegar ao final desse projeto de mestrado não foi fácil. Surgiram grandes obstáculos profissionais no caminho, problemas de saúde, perdi pessoas queridas e passamos por muitos problemas em campo. Ainda assim, devido às tantas incertezas que as mudanças climáticas colocam sobre o nosso futuro e à paixão que tenho pela ciência, sinto uma obrigação pessoal em entregar um trabalho que desenvolva o conhecimento da melhor maneira que eu consiga.

Profissionalmente, preciso agradecer aos meus orientadores, David Lapola e Martin De Kauwe, que me possibilitaram chegar até o final com algumas respostas para as perguntas que fazíamos a três anos atrás, enquanto elaborávamos a ideia. Obrigado por todos os momentos de reunião e conselhos profissionais que foram essenciais para que tudo acontecesse. Também agradeço a todos os professores que tive durante o curso de ecologia quantitativa do Instituto Serrapilheira, que me fizeram enxergar a Ecologia de uma forma totalmente diferente da que eu estava acostumado. Isso foi muito importante para eu conseguir fazer o melhor possível com o que estava disponível.

Pessoalmente, não posso deixar de agradecer aos meus pais, a todos os meus amigos do LabTerra e, principalmente, aos meus amigos da Biologia Unicamp, que sempre estiveram comigo para deixar as coisas mais leves nos momentos de quase desistência desde 2018. Não é todo mundo que entende as nossas ambições e dificuldades como biólogos e cientistas, e sem vocês eu sei que não teria chegado até aqui.

Agradeço também a todos os amigos que a música eletrônica me deu ao longo desses anos encontrando o meu lugar como artista. Explorar a arte, para mim, geralmente é um caminho solitário, e fazer parte de uma comunidade de pessoas que entendem essa jornada é libertador. Obrigado por todos os momentos juntos e pela música que vocês colocam no mundo.

Agradeço à Fundação de Amparo à Pesquisa do Estado de São Paulo (FAPESP, processo nº 2021/14348-5) pelo financiamento majoritário deste trabalho. O presente trabalho foi realizado com apoio da Coordenação de Aperfeiçoamento de Pessoal de Nível Superior - Brasil (CAPES) - Código de Financiamento 001.

# Resumo

As mudanças climáticas do Antropoceno têm o potencial de alterar profundamente as dinâmicas da biosfera. Os efeitos específicos dessas mudanças em cada ecossistema, no entanto, não são previsíveis, devido à longa série de dependências e interações entre componentes desse sistema complexo. Para a vegetação da Floresta Amazônica, a situação não é diferente: as respostas ainda não são bem conhecidas, especialmente quando o enfoque não é apenas no dossel. Há uma grande necessidade de esclarecer a influência do aumento de CO<sub>2</sub> nos diferentes estratos da floresta. Dessa forma, o presente estudo tem como objetivo elucidar, as respostas da transpiração de plantas do sub-bosque da Amazônia Central em relação aos crescentes níveis de CO<sub>2</sub> na atmosfera. Para cumprir tal objetivo, foram avaliadas as trocas gasosas de plantas de floresta nativa sujeitas a níveis elevados de CO<sub>2</sub> crescendo no interior de câmaras de topo aberto através de medições em campo e de estimativas feitas por modelos matemáticos, possibilitando uma classificação fisiológica das medidas obtidas. Os resultados obtidos não indicam diferenças significativas entre indivíduos crescendo em concentrações ambiente de CO<sub>2</sub> e em concentrações elevadas. Apesar disso, foi observada uma alta diversidade intraespecífica de capacidade fotossintética, com uma evidente diferença de estratégia de uso de água entre as duas espécies dominantes de sub-bosque avaliadas. Tal diferença, em conjunto com a grande variabilidade encontrada, sugere a possibilidade de que mudanças na composição da comunidade sejam observadas em resposta a mudanças nas condições climáticas. Ainda assim, devido ao fato de que o ecossistema possui uma grande diversidade de espécies e possíveis estratégias de uso de água, uma maior quantidade de dados é necessária para a compreensão das prováveis mudanças que poderão ocorrer no sub-bosque da Floresta Amazônica nas próximas décadas.

# Abstract

Climate change in the Anthropocene has the potential to profoundly alter the dynamics of the biosphere. The specific effects of these changes in each ecosystem, however, are unpredictable due to the complex interdependencies and interactions among system components. The same is true for the vegetation of the Amazon Rainforest: the responses are still not well understood, especially when the focus is below the canopy. There is a great need to clarify the impact of increased CO<sub>2</sub> on the different forest layers. Therefore, this study aims to elucidate the responses of understory plant transpiration to rising atmospheric CO<sub>2</sub> levels in Central Amazon. To achieve this, we evaluated the gas exchanges of native forest plants exposed to elevated CO<sub>2</sub> levels in open-top chambers through field measurements and mathematical model estimates, allowing for a physiological classification of the obtained data. The results did not indicate significant differences between individuals growing in ambient CO<sub>2</sub> concentrations and those in elevated CO<sub>2</sub> concentrations. Despite this, we observed high intraspecific diversity in photosynthetic capacity and a clear difference in water use strategies between the two dominant understory species evaluated. This difference, along with the high variability found, suggests potential community shifts regarding the studied species in response to changing climatic conditions. However, due to the ecosystem's vast diversity of species and possible water use strategies, more data is needed to understand the likely changes that may occur in the Amazon Rainforest understory in the coming decades.

# List of Figures

|      |  |    |
|------|--|----|
| 3.1  | OTC example . . . . .  | 20 |
| 4.1  | PAR measurements recorded by meteorological tower . . . . .  | 28 |
| 4.2  | Response curvature (theta) estimates for experimental groups . . . . .   | 29 |
| 4.3  | Response curvature (theta) estimates for species . . . . .   | 29 |
| 4.4  | Quantum Yield estimates for experimental groups . . . . .  | 30 |
| 4.5  | Quantum Yield estimates for species . . . . .  | 30 |
| 4.6  | Vcmax estimates for experimental groups . . . . .  | 31 |
| 4.7  | Vcmax estimates for species . . . . .  | 31 |
| 4.8  | Jmax estimates for experimental groups . . . . .   | 32 |
| 4.9  | Jmax estimates for species . . . . .   | 32 |
| 4.10 | Rd estimates for experimental groups . . . . .   | 33 |
| 4.11 | Rd estimates for species . . . . .   | 33 |
| 4.12 | $g_1$ variable $g_k$ model values for A/RH curves by experimental group . . . .                                | 34 |
| 4.13 | $g_1$ variable $g_k$ model values for A/RH curves by species . . . . .   | 35 |
| 4.14 | $g_1$ fixed $g_k$ model values for A/RH curves by experimental group . . . . .                                 | 35 |
| 4.15 | $g_1$ fixed $g_k$ model values for A/RH curves by species . . . . .  | 36 |
| 4.16 | $g_k$ values for A/RH curves . . . . .   | 36 |
| 4.17 | $g_k$ values for A/RH curves . . . . .   | 37 |
| 4.18 | Stomatal conductance measurements for experimental groups . . . . .  | 39 |
| 4.19 | Stomatal conductance measurements for species . . . . .  | 39 |
| 4.20 | Stomatal conductance measurements separated by humidity intervals . . . .                                      | 40 |
| 4.21 | Transpiration scaled-up data divided by experimental group . . . . .   | 41 |
| 4.22 | Transpiration scaled-up data divided by species . . . . .  | 42 |
| 4.23 | Transpiration scaled-up data divided by experimental group and species . .                                     | 42 |
| 4.24 | Transpiration scaled-up data adjusted for leaf area and divided by<br>experimental group . . . . .             | 43 |
| 4.25 | Transpiration scaled-up data adjusted for leaf area and divided by species .                                   | 43 |
| 4.26 | Transpiration scaled-up data adjusted for leaf area and divided by<br>experimental group and species . . . . . | 44 |
| A.1  | Stomatal conductance A/Ci measurements by experimental groups . . . . .  | 58 |
| A.2  | Stomatal conductance A/Ci measurements by species . . . . .  | 59 |
| A.3  | Stomatal conductance A/Q measurements by experimental groups . . . . .   | 59 |
| A.4  | Stomatal conductance A/Q measurements by species . . . . .   | 60 |
| A.5  | Jmax/Vcmax ratio per experimental groups . . . . .   | 61 |
| A.6  | Jmax/Vcmax ratio per species . . . . .   | 61 |
| A.7  | A/Q response curve example . . . . .   | 62 |
| A.8  | A/Ci response curve example . . . . .  | 62 |
| A.9  | Stomatal conductance response to CO2 example . . . . .   | 63 |

|   |    |
|---|----|
| A.10 A/RH response curve example . . . . .  | 63 |
| A.11 A/RH response curves data . . . . .  | 64 |
| A.12 Individual leaf area divided by experimental group . . . . .   | 65 |
| A.13 Individual leaf area divided by species . . . . .  | 65 |
| A.14 Individual leaf area divided by experimental group and species . . . . .                               | 66 |
| A.15 Net assimilation scaled-up data divided by experimental group and species                              | 67 |
| A.16 Stomatal conductance scaled-up data divided by experimental group and<br>species . . . . .             | 67 |
| A.17 Transpiration scaled-up data for fixed gk model divided by experimental<br>group . . . . .             | 68 |
| A.18 Transpiration scaled-up data for fixed gk model divided by species . . . . .                           | 68 |
| A.19 Transpiration scaled-up data for fixed gk model divided by experimental<br>group and species . . . . . | 69 |

# List of Tables

|     |  |    |
|-----|--|----|
| 3.1 | Values for the varying controlled variables sequences of each of the three types of response curves conducted during the study. . . . .  | 23 |
| A.1 | Confounding factors significance - Model formulas and p-value results for species, experimental groups, relative growth rate ( <i>rgr</i> ) and soil water content ( <i>wsoil</i> ). . . . .           | 57 |
| A.2 | Leaf area (in square meters) for experimental groups and species is presented alongside the total leaf area of all individuals within the OTCs. Data from outside control groups is not shown. . . . . | 58 |

# List of Symbols

|                  |   |
|------------------|---|
| IRGA             | Infrared gas analyzer                           |
| OTC              | Open-top chamber                                |
| FACE             | Free-air concentration enrichment               |
| A                | Net CO <sub>2</sub> assimilation rate           |
| RH               | Air relative humidity                           |
| Q                | Irradiance                                      |
| C <sub>i</sub>   | Substomatal CO <sub>2</sub> concentration       |
| A/C <sub>i</sub> | Photosynthetic carbon dioxide response curve    |
| A/Q              | Photosynthetic light response curve             |
| A/RH             | Photosynthetic relative humidity response curve |
| eCO <sub>2</sub> | Elevated carbon dioxide concentration           |
| aCO <sub>2</sub> | Ambient carbon dioxide concentration            |
| LAI              | Leaf area index                                 |
| PAR              | Photosynthetically active radiation             |

# Contents

|          |   |           |
|----------|---|-----------|
| <b>1</b> | <b>Introduction</b>   | <b>15</b> |
| <b>2</b> | <b>Objectives and hypotheses</b>  | <b>18</b> |
| <b>3</b> | <b>Materials and Methods</b>  | <b>20</b> |
| 3.1      | Experimental site . . . . .   | 20        |
| 3.1.1    | Location . . . . .  | 20        |
| 3.1.2    | Plot design . . . . .   | 21        |
| 3.1.3    | Micrometeorological tower . . . . .                                     | 21        |
| 3.2      | Plant species . . . . .   | 21        |
| 3.3      | Gas exchange curves . . . . .   | 22        |
| 3.4      | Confounding factors . . . . .   | 23        |
| 3.4.1    | Soil moisture and leaf surface temperature . . . . .                    | 23        |
| 3.4.2    | Relative growth rate (RGR) . . . . .                                    | 24        |
| 3.5      | Leaf area . . . . .   | 24        |
| 3.6      | Mathematical models . . . . .   | 24        |
| 3.6.1    | Model for A/Ci curve fitting . . . . .                                  | 25        |
| 3.6.2    | Photosynthesis light response (A/Q) . . . . .                           | 25        |
| 3.6.3    | Stomatal conductance model . . . . .                                    | 25        |
| 3.7      | Statistical analysis . . . . .  | 26        |
| 3.8      | Big-leaf estimation . . . . .   | 26        |
| <b>4</b> | <b>Results</b>  | <b>28</b> |
| 4.1      | Understory light availability . . . . .                                 | 28        |
| 4.2      | Gas exchange measurements . . . . .                                     | 28        |
| 4.2.1    | Marshall-Biscoe parameters (A/Q) . . . . .                              | 28        |
| 4.2.2    | Farquhar model parameters (A/Ci) . . . . .                              | 30        |
| 4.2.3    | Medlyn parameters . . . . .   | 34        |
| 4.2.4    | Curve fits . . . . .  | 38        |
| 4.3      | Stomatal conductance measurements . . . . .                             | 38        |
| 4.4      | Big-leaf model . . . . .  | 41        |
| 4.4.1    | Estimated results without the inclusion of leaf area . . . . .          | 41        |
| 4.4.2    | Estimated results including leaf area . . . . .                         | 42        |
| <b>5</b> | <b>Discussion</b>   | <b>45</b> |
| <b>6</b> | <b>Conclusion</b>   | <b>48</b> |
|          | <b>References</b>   | <b>50</b> |
| <b>A</b> | <b>Appendix</b>   | <b>57</b> |
| A.1      | Additional tables . . . . .   | 57        |
| A.2      | Stomatal conductance measurements from A/Ci and A/Q curves . . . . .    | 58        |
| A.3      | $J_{max} / V_{cmax}$ ratio plots . . . . .                              | 61        |
| A.4      | Examples of response curves measured at the experimental site . . . . . | 62        |
| A.5      | Individual leaf area . . . . .  | 65        |
| A.6      | Big leaf upscaling: additional plots . . . . .                          | 66        |

|     |  |    |
|-----|--|----|
| A.7 | Declaration of copyright . . . . .               | 70 |
| A.8 | Declaration of bioethics and biosafety . . . . . | 71 |

# Introduction

Climate and environmental changes have the potential to shape the state of ecosystems and the entire world (IPCC, 2023; GISSI et al., 2021). Throughout the history of life on Earth, these shifts have unfolded over geological timescales, gradually molding the intricate relationships between biotic and abiotic elements across millennia (YU; RAYNOLDS, 2024). With the human interferences which characterize the Anthropocene, the rate of change has dramatically increased. The rise in CO<sub>2</sub> levels in recent centuries is estimated to be up to 10 times faster than the most abrupt changes in the past 100 million years (RAE et al., 2021), leaving a small time frame for the ecosystems to adapt. These steep changes, evident in different forms across all ecosystems on Earth (BAZZAZ, 1990), are created by the actions of modern society and reverberate throughout society itself, due to the potentially global consequences of such impacts (IPCC, 2023).

On plant communities worldwide, which provide the basal trophic level of most terrestrial ecosystems, the effects of these changes are the subject of extensive debate in the scientific community. Regarding the rise of atmospheric CO<sub>2</sub> concentrations, the limited amount of studies conducted in rainforests report few changes in plant physiology that vary between species (WÜRTH; WINTER; KÖRNER, 1998), whereas experiments in temperate ecosystems reveal significant impacts on plant communities (JIANG et al., 2020). In general, plant response to CO<sub>2</sub> increase is not linear and affected solely by the gas concentration itself, but rather dependent on the conditions of each ecosystem and the species involved (WÜRTH; WINTER; KÖRNER, 1998; OLIVEIRA et al., 2012; LAMOUR et al., 2022). For the understory of tropical rainforests, the stratum of the ecosystem that is the focus of this study, the effects are still poorly understood, making it challenging to define solid predictions for the future of rainforests in the coming decades (OLIVEIRA et al., 2012).

Among the several physiological aspects of the plant community that can be altered by increased CO<sub>2</sub> concentrations (ZELIKOVA et al., 2014; WANG et al., 2012; NEWINGHAM et al., 2014), the flux of water from the plants to the atmosphere, mainly through stomatal transpiration, is the central aspect of this study. Jiménez-Rodríguez et al. (2020) demonstrated that the rainforest understory in Costa Rica can contribute up

to 24% of total evaporation, highlighting the significance of responses in this stratum for overall water flux. Changes in this process have the potential to influence the precipitation on a continental scale, affecting biome composition and processes, and, when viewed as an ecosystem service issue, impacting water availability, crop production, and thermal regulation (LIMA et al., 2014).

Studies reporting stomatal response to CO<sub>2</sub> can be traced back to the 1940s in the literature (ZEIGER; FARQUHAR; COWAN, 1987; MORISON, 1998). However, *in situ* studies reporting responses to elevated CO<sub>2</sub> comparable to modern measurements were only published in the 1990s, enabled by gas exchange chamber technology (KAPPEN; ANDRESEN; LOSCH, 1987). These studies present a high emphasis on temperate biomes (ALENCAR et al., 2024; AINSWORTH; LONG, 2005), although some studies in the tropics can be found (WÜRTH; WINTER; KÖRNER, 1998). Due to this research history of the past decades, the measured response of the Amazon rainforest to eCO<sub>2</sub> is still unknown, and can be dependent on several factors, such as nutrient availability, water limitation and biotic interactions (LIN et al., 2015; XU; JIANG; JIA, et al., 2016). Therefore, providing data on hyperdiverse rainforest regions like the Amazon is crucial for understanding how these ecosystems will respond to predicted changes in the coming decades (FLEISCHER et al., 2019).

As mentioned before, scientists have been describing leaf stomatal responses to environmental conditions for several decades. Some core aspects of the system are considered general responses, such as the aperture reduction of stomata in higher CO<sub>2</sub> concentrations, but it is important to differentiate general responses from universal responses (XU; JIANG; JIA, et al., 2016). The dynamic and complex environment created by natural ecosystems demands that plants acclimate to changes and behave differently according to the available resources. A clear example of this is the stomatal behavior during water limitation, where the closure is more pronounced, to the extent that soil water availability is considered the most influential environmental factor on stomatal aperture (XU; JIANG; ZHOU, 2015). When taking these points into account in the Amazon understory, it is possible that the responses vary widely from those observed in temperate forests, as basic environmental conditions such as air temperature, soil humidity, air relative humidity and light availability are distinct, creating a forest stratum where most of the data collected in this topic does not directly translate (HUBAU et al., 2019).

In order to conduct an experiment that exposes whole plants to eCO<sub>2</sub>, there are essentially two types of designs commonly used in science: a chamber where enriched air circulates through the plants (Open-Top Chamber, OTC) or a series of pipes that disperse enriched air across an open area (Free Air CO<sub>2</sub> Enrichment, FACE). These methods, each having its own benefits over the other (MACHÁČOVÁ, 2010), provide consolidated strategies to test the impacts of eCO<sub>2</sub> on the plants, and form the structural basis for the studies conducted by the AmazonFACE program, which this study is part of. The methodology presented here was conducted in an OTC experimental setting, suitable for conducting an understory study.

The use of the aforementioned structures for in situ experiments in hyperdiverse tropical ecosystems is still scarce in the literature (ALENCAR et al., 2024; BARLOW et al., 2018). In Latin America, only three OTC experiments fitting this description have been conducted (WÜRTH; WINTER; KÖRNER, 1998; BADER et al., 2022), including the one being conducted by AmazonFACE (LAPOLA; NORBY, 2014; AMAZONFACE, 2024). As for FACE experiments, it has still never been done. The hyperdiversity of the ecosystem can influence the responses observed in previous studies in several manners (TURNER; BRENES-ARGUEDAS; CONDIT, 2018; HE; BAZZAZ; SCHMID, 2002), another way in which the tropical environmental forces differ widely from the conditions present in previous study sites, such as the Duke forest from FACE US (OREN et al., 2006; MAIER et al., 2022) and the eucalyptus forest used for EucFACE in Australia (JIANG et al., 2020). It is also expected that the responses from the rainforest canopy will differ from those already known for the understory (ARNONE; KÖRNER, 1993), providing another factor of uncertainty and underscoring the necessity of conducting this type of experiment in the tropics.

Many aspects of the plant community can be evaluated using an OTC experiment. With the present study, we aim to shed light on the effects of CO<sub>2</sub> on the plant-atmosphere water flux in the chambers, while also providing physiological data to characterize the species studied at the site. This will allow us to provide insights into how the simulated elevated CO<sub>2</sub> levels can alter the community, potentially influencing diversity factors such as dominance and intraspecific diversity, as well as the contribution of the community to precipitation in the Amazon basin. As shown before, there is a historical lack of data for the tropics on this topic, an issue that the AmazonFACE program aims to address.

# Objectives and hypotheses

The measurements presented here can provide the necessary data to determine if the exposure to elevated CO<sub>2</sub> concentrations during a time frame of four months can alter the stomatal response of understory plants from the Central Amazon. The estimations generated by upscaling these responses can, in turn, provide insights on how the climate along a longer time period affects the instantaneous responses observed in the field. Specifically, the main goals of this study are presented below:

## Main goals:

- Evaluate the short-term effects of elevated CO<sub>2</sub> on the Central Amazon understory vegetation-atmosphere water flux;
- Investigate the effectiveness of the stomatal conductance model utilized in this study to represent plant response to CO<sub>2</sub> in the Amazon understory.

## Hypotheses

Based on the insights gained from the literature review and prior observations at the experimental site, we propose two hypotheses to address our central research question: What are the short-term effects of elevated CO<sub>2</sub> on the water flux between the vegetation and atmosphere in the Central Amazon understory? Our hypotheses are:

### Hypothesis 1 - Modeling background

The physiological models describing stomatal response to increased CO<sub>2</sub> support the assumption that a rise in concentration will result in a reduction in stomatal conductance for the same amount of carbon assimilated in photosynthesis. From this point of view, it is reasonable to expect that a consistent reduction in stomatal conductance for the treatment experimental group when compared to control values.

### Hypothesis 2 - Understorey response background

The scarce literature on stomatal response in the understory of rainforests, when combined with the knowledge of review papers for this type of elevated CO<sub>2</sub> experiment, suggests that CO<sub>2</sub> concentration is not a strong response driver in this relationship, being more

influenced by other abiotic and biotic factors, such as soil water content, luminosity, air relative humidity and pathogen vulnerability. In this case, we would expect no consistent differences to be observed between experimental groups.

# Materials and Methods

## 3.1 Experimental site

### 3.1.1 Location

The study site, located at the Experimental Station of Tropical Forestry (EEST/ZF-2, Manaus), is maintained and monitored by the National Institute for Amazonian Research (INPA), as part of the LBA (Large Scale Biosphere-Atmosphere Research Program in the Amazon) program. The site is also hosting the Amazon Free-Air CO<sub>2</sub> Enrichment program (AMAZONFACE, 2024), which the experimental structure used in this study is part of. The vegetation from the site is characterized as a highly diverse upland (*terra firme*) rainforest, with an average canopy height of 30 m (PEREIRA et al., 2019). The light availability during the daytime is usually close to 25  $\mu\text{mol m}^{-2} \text{s}^{-1}$ , with the occasional sunflecks providing much more intense irradiance for brief periods of time (Fig. 4.1). The mean annual precipitation at the station, measured by the K34 tower equipment, is 2400 mm, with monthly values ranging from 80 to 400 mm (TANAKA; SATYAMURTY; MACHADO, 2014; DAMASCENO et al., 2024).



**Figure 3.1:** Photograph showing one of the OTCs and the tarp barrier placed on the soil.

### 3.1.2 Plot design

At the experimental site, 12 circular plots were installed, where each individual is monitored. The soil from the plots is isolated from the adjacent soil by a 30 x 50 cm tarp barrier buried in the perimeter. Of the 12 plots, 8 have an open-top chamber installed, measuring 2.5 m in diameter and 3 m in height, sufficient to accommodate small arboreal individuals from the understory. The chambers are ventilated by a lateral fan and the CO<sub>2</sub> concentration is regulated by a pressurized cylinder automated system, maintaining the treatment concentration 250 ppm above ambient levels during daytime. The experiment was built in a coupled design, meaning that the plots are grouped in triads, with a treatment, control and outside control (without an OTC) plot close to each other. Apart from the demographic aspects of the experiment, such as leaf count and growth rate, CO<sub>2</sub> concentration and luminosity values are constantly measured, the former by an infrared gas analyser (LI-840A, Li-Cor Inc., Lincoln, USA) and the latter by quantum meters. The increased CO<sub>2</sub> treatment, during the whole execution of the OTC experiment, have been turned on and off due to equipment malfunctions and maintenance several times. For the purpose of this study, with all response curves collected between 29/06/2023 and 22/07/2023, the treatment OTCs were subjected to increased CO<sub>2</sub> levels since March 2023.

### 3.1.3 Micrometeorological tower

A micrometeorological tower, in use since 2019, is also installed on the site. Among the several variables and height levels monitored, it provides data at 3.3 m height for the air temperature, luminosity, and relative humidity, which will be important for the present study during the model temporal upscaling process. During the period used for that purpose, the mean relative humidity in the understory stratum was 94.64 %, while the light intensity is shown in figure 4.1.

## 3.2 Plant species

The two species chosen for the present study are *Duguetia flagellaris* Huber and *Paypayrola grandiflora* Tul., both of which are abundant arboreal understory species in the experimental site and the most dominant in the plots. When combined, these

species are present in all 12 plots, representing the selection with the fewest possible species, as no single species is present in all plots. By limiting the analysis to only two presumably functionally similar species, we expected to reduce interspecific variability and uncertainties. Each of the 37 individuals had one of their leaves measured with a portable photosynthesis system with a leaf chamber infrared gas analyser (LI-6400XT, Li-Cor Inc. Lincoln, USA) for carbon assimilation and stomatal conductance under three different varying conditions: varying luminosity (A/Q response), CO<sub>2</sub> concentration (A/Ci response) and relative humidity (A/RH response). The fully expanded leaves used for the response curve also had their surface temperatures at the beginning of each curve measured with an infrared thermometer. Due to the limited amount of days in the field available, it was only possible to measure the response of one leaf per individual for each type of curve. Dominance in terms of leaf area can be consulted in table A.2.

### 3.3 Gas exchange curves

All field measurements regarding the photosynthesis response curves and possible confounding variables were obtained between June and July 2023, corresponding to the beginning of the dry season in the region. The response curve protocol for the three types of curves conducted during the study is to maintain constant chamber conditions, while varying one of the variables in order to see how the variables measured by the IRGA (H<sub>2</sub>O vapor and CO<sub>2</sub> concentrations) behave. For the A/Q curve, the relative humidity was maintained, on average, at 70%; the CO<sub>2</sub> concentration was 400 ppm for all curves, the leaf temperature was maintained at 30°C and the PAR was controlled following the sequence shown in table 3.1. For the other two types of curves, the PAR was maintained at 1000  $\mu\text{mol m}^{-2} \text{s}^{-1}$ , as this value was enough to saturate the A/Q response curves for the individuals. The chamber air flow rate was maintained at 400  $\mu\text{mol s}^{-1}$  for all curves, except for the A/RH at the higher humidity points, where flow sometimes had to be reduced to achieve the values. The sequence of values used for the A/Ci and A/RH response curves can also be found in table 3.1, while examples of each measurement sequence are presented in the appendix, figures A.7 to A.11. The measurement protocol and variable sequences here described were adapted from Menezes et al. (2022) and Damasceno et al. (2024).

**Table 3.1:** Values for the varying controlled variables sequences of each of the three types of response curves conducted during the study.

| A-Q PAR values ( $\mu\text{mol}$ ) | A-Ci CO2 values (ppm) | A-RH RH values (%) |
|------------------------------------|-----------------------|--------------------|
| 250                                | 400                   | 85                 |
| 500                                | 200                   | 70                 |
| 750                                | 100                   | 55                 |
| 100                                | 75                    | 40                 |
| 1500                               | 50                    | 25                 |
| 500                                | 0                     | 10                 |
| 250                                | 400                   |                    |
| 100                                | 600                   |                    |
| 75                                 | 800                   |                    |
| 50                                 | 1000                  |                    |
| 25                                 | 1200                  |                    |
| 10                                 | 1500                  |                    |
| 5                                  | 1800                  |                    |
| 0                                  | 2000                  |                    |

### 3.4 Confounding factors

In order to account for the several varying conditions between the OTCs, some of the possible variables that could interfere with the results were also taken into account while in the field and during data analysis. These factors were: average soil moisture within the OTCs, leaf surface temperature, and plant relative growth rate. The significance of these factors with the results are shown in table A.1.

#### 3.4.1 Soil moisture and leaf surface temperature

The soil moisture of the chambers was estimated at the beginning of each set of measurements in the OTCs. The estimation was obtained by calculating the mean value of five measurement points within the perimeter: four opposing points near the borders and one central point, all at a depth of 5 cm. The data, collected with a soil moisture sensor (SM150 Kit, Delta-T Devices, Cambridge, UK), were used during the statistical analysis, in order to test if differences in humidity would influence the comparison of observed results. The temperature of the leaf at the beginning of each gas exchange measurement was determined using an infrared thermometer.

### 3.4.2 Relative growth rate (RGR)

The physical aspects of the plants monitored inside the OTCs, such as leaf count and height, are measured during demography field campaigns. RGR is calculated based on the difference in height of the plants in relation to the previous data. This variable was used in the statistical analysis to assess if these differences would influence the comparison between the observed results.

## 3.5 Leaf area

Leaf area index (LAI) of the understory vegetation close to each chamber was estimated via paired hemispherical images, taken with a Canon Rebel EOS T3 camera coupled with a Sigma 8 mm lens, with one picture taken at 3 m height and the other at 1 m height. The LAI estimation was obtained by subtracting the higher picture estimation from the lower one, representing the leaf area index for the vegetation between both heights. The estimations were processed using the R package *hemispheR* (CHIANUCCI; MACEK, 2024). In order to obtain the average leaf area inside the OTCs, data from a previous field campaign in 2020 was utilized (DAMASCENO et al., 2024). This measurement was important for upscaling the stomatal conductance data, as conducting another manual leaf area measurement during the available field period was not feasible. While an estimation could be made using the collected LAI data, using the actual measurements inside the chambers provides a more accurate estimation (data shown in table A.2).

## 3.6 Mathematical models

In order to evaluate the obtained measurements, three models consolidated in the plant physiology and modeling scientific community were used during this study, which were crucial to obtain parameter values regarding the response of the individuals in relation to light availability, CO<sub>2</sub> concentration and humidity.

### 3.6.1 Model for A/Ci curve fitting

The fit for the A/Ci curves was done using the function *fit\_aci\_response* from the R package *photosynthesis* (STINZIANO et al., 2023) function designed for this estimation, which is based on Gu et al. (2010) and Bernacchi et al. (2001), papers that build upon the original model from Farquhar, Caemmerer, and Berry (1980), providing the following main parameters:  $V_{cmax}$  ( $\mu\text{mol m}^{-2} \text{s}^{-1}$ ), the maximum RuBP saturated carboxylation rate;  $J_{max}$  ( $\mu\text{mol m}^{-2} \text{s}^{-1}$ ), maximum electron transport rate;  $\Gamma$  (Pa), the  $\text{CO}_2$  compensation point of photosynthesis and  $R_d$  ( $\mu\text{mol m}^{-2} \text{s}^{-1}$ ), the dark respiration. For the purposes of the present study, the focus is on  $V_{cmax}$  and  $J_{max}$  values and their distribution across the experimental groups and individuals.

### 3.6.2 Photosynthesis light response (A/Q)

The model parameters related to the light response of net  $\text{CO}_2$  assimilation  $A_n$  were estimated using the equation from Marshall and Biscoe (1980), which, similarly to the Farquhar model, has been integrated into the *photosynthesis* R package. The non-rectangular hyperbola model equation and its parameters are presented below:

$$A_{max} + R_d = \frac{\phi I (A_{max} - \theta A_n)}{(1 - \theta)\phi I + (A_{max} - \theta A_n)} \quad (3.1)$$

where  $I$  is the irradiance,  $R_d$  is the dark respiration rate,  $A_{max}$  the maximum rate of net photosynthesis,  $\phi$  is the photochemical efficiency of photosynthesis at low light (quantum yield) and  $\theta$  is the curvature of the response, which represents the ratio of physical to total resistance to diffusion of  $\text{CO}_2$ .

### 3.6.3 Stomatal conductance model

The stomatal conductance parameters were estimated using the unified stomatal model described by Medlyn, Duursma, Eamus, et al. (2011), employing non-linear fitting algorithms in R. The equation and the estimated parameters are presented below:

$$g_s \approx g_0 + 1.6 \left( 1 + \frac{g_1}{D^{g_k}} \right) \frac{A}{C_a} \quad (3.2)$$

where  $g_s$  ( $\text{mol m}^{-2} \text{s}^{-1}$ ) is the estimated stomatal conductance,  $D$  (kPa) is the vapor pressure deficit,  $A$  ( $\mu\text{mol m}^{-2} \text{s}^{-1}$ ) is the net assimilation rate, and  $C_a$  is the ambient

CO<sub>2</sub> concentration ( $\mu\text{mol mol}^{-1}$ ). The estimated parameters are  $g_1$ , the conductance sensitivity to  $D$  and  $A$  ( $\text{kPa}^{g_k}$ );  $g_0$ , the residual stomatal conductance ( $\text{mol m}^{-2} \text{s}^{-1}$ ); and  $g_k$ , conductance sensitivity to  $D$  ( $\text{kPa}^{-1}$ ).

In this model,  $g_k$  is supposed to be  $0.5 \text{ kPa}^{-1}$  when assuming the stomatal behavior to be optimal, meaning that the carbon gain should be maximized, while minimizing the loss of water. However, this assumption is debatable, even more in eCO<sub>2</sub> conditions (MEDLYN; DUURSMA; EAMUS, et al., 2011; MEDLYN; DUURSMA; DE KAUWE, et al., 2013). Regarding the conductance sensitivity to vapor pressure deficit and carbon assimilation, represented by the parameter  $g_1$ , the following proportion is linked to the parameter:

$$g_1 \propto \sqrt{\Gamma^* \lambda} \quad (3.3)$$

where  $\Gamma^*$  is the CO<sub>2</sub> compensation point and  $\lambda$  is the marginal water cost of carbon.

### 3.7 Statistical analysis

The equations were used to analyze the measurements of each individual, generating non-linear regressions for the data and its parameters. These parameters were then employed to assess the effects of the experiment on the two species studied. Statistical comparisons of the differences were conducted using either the Wilcoxon test for interspecies comparisons or post-hoc ANOVA for comparisons among experimental groups, as depicted in the figures. Initially, potential confounding factors measured in the field were incorporated into the statistical analysis. However, none of these factors affected the observed results, hence the simplest statistical models were retained for this analysis.

### 3.8 Big-leaf estimation

The obtained model parameters were also used to feed a big-leaf simulation script, which employed the same equations applied to the field data combined with the Penman-Monteith equation (LEUNING et al., 1995) to estimate stomatal conductance, carbon assimilation, and transpiration values under different meteorological conditions,

inputted from the data provided from the sensors installed at the site. These estimations were also used to compare the response of the different experimental groups and species, adjusted to the leaf area from each OTC, providing a comparison during a longer period of time. The environmental variables used for this purpose were the light intensity and the relative humidity at the height of 3.3 m, in a time series from January 2019 to February 2019 only due to data quality limitations. As trying longer periods returned no different results, the decision was to keep the results for this time period only, and maintaining this specific period ensured the quality of the data.

# Results

## 4.1 Understory light availability

To contextualize the dynamics of light availability in the understory stratum, luminosity data from the quantum sensors installed on the meteorological tower are presented here in figure 4.1. It is evident that the average light availability is quite low, forcing the plant community to rely on random, short spikes of high luminosity, known as sunflecks.

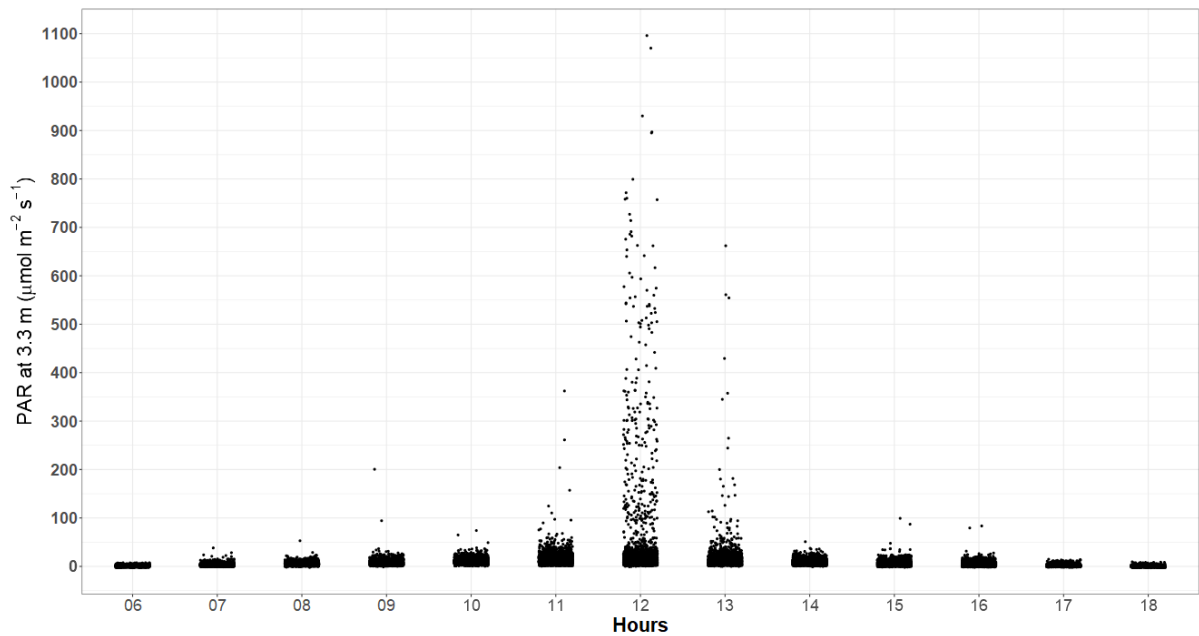


**Figure 4.1:** Photosynthetically Active Radiation (PAR) measurements recorded by the micrometeorological tower over a two-month period, categorized by hourly intervals throughout the day.

## 4.2 Gas exchange measurements

### 4.2.1 Marshall-Biscoe parameters (A/Q)

Presented here are the boxplots showing the parameters obtained from the Marshall and Biscoe (1980) model, applied on the light response (A/Q) curves measured in the field. The response curvature and quantum yield estimates were used as inputs into the Gu et al. (2010) model in order to provide a more reliable estimation. Regarding the

Marshall-Biscoe model parameters, no significant differences between groups have been observed, although a high variance is present for groups.

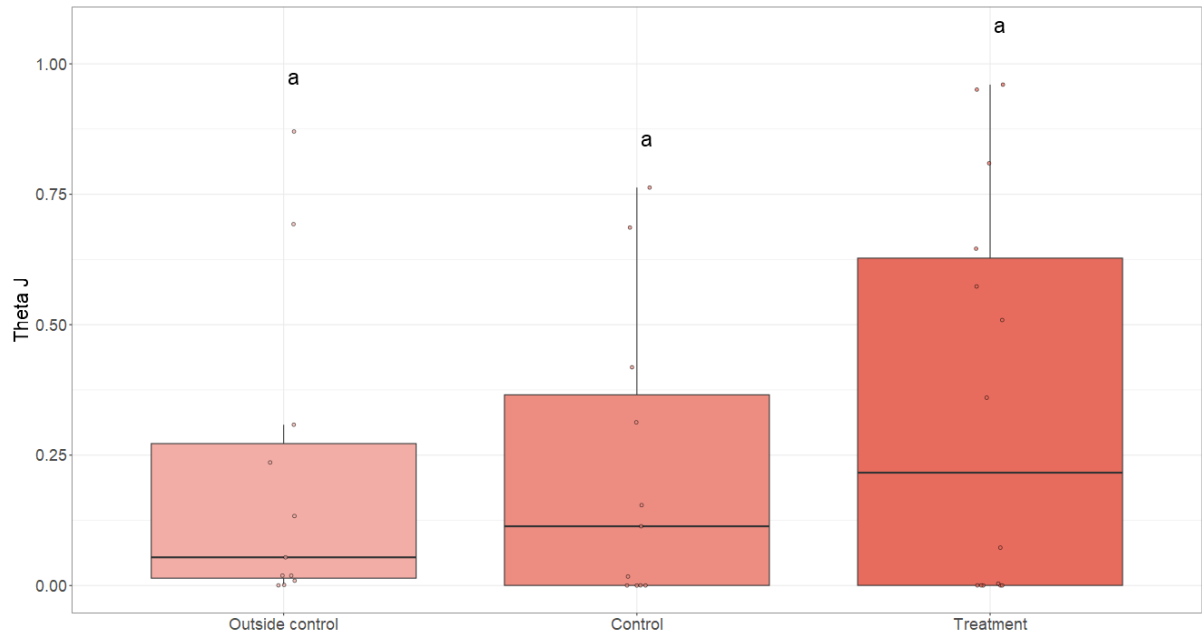


**Figure 4.2:** Boxplot showing the response curvature (theta) separated between the three experimental groups of the study. The letters above each boxplot show the Tukey test results, indicating whether there is a significant difference between the groups.

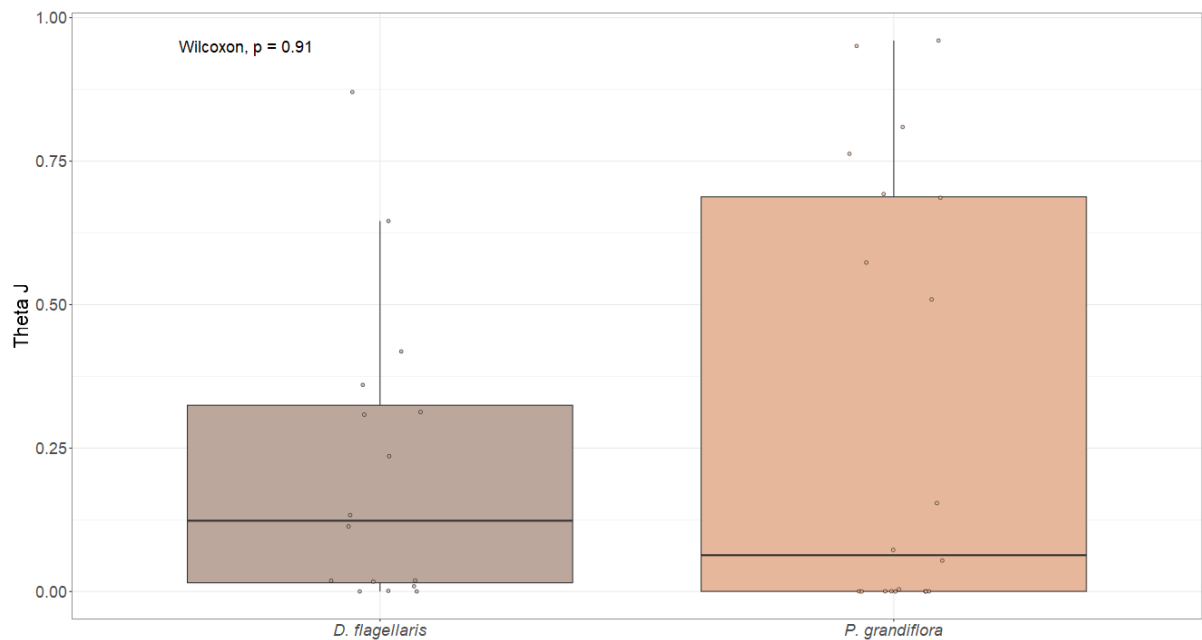


**Figure 4.3:** Boxplot showing the response curvature (theta) separated between the two species used in the study.

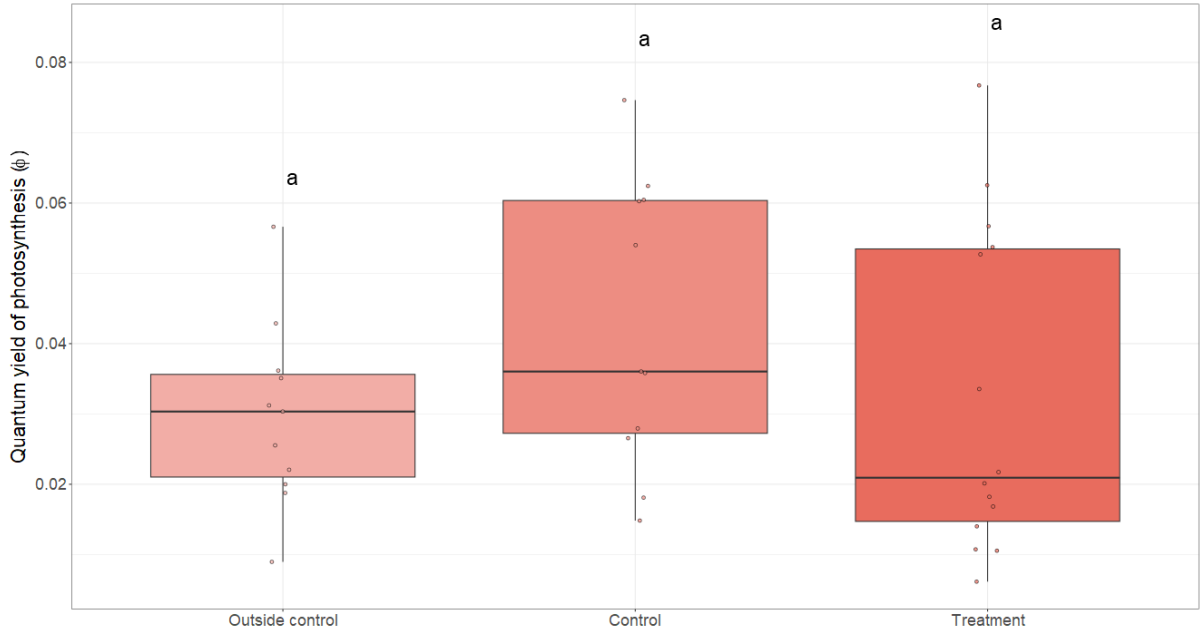


**Figure 4.4:** Boxplots showing the quantum yield estimates separated between experimental groups.

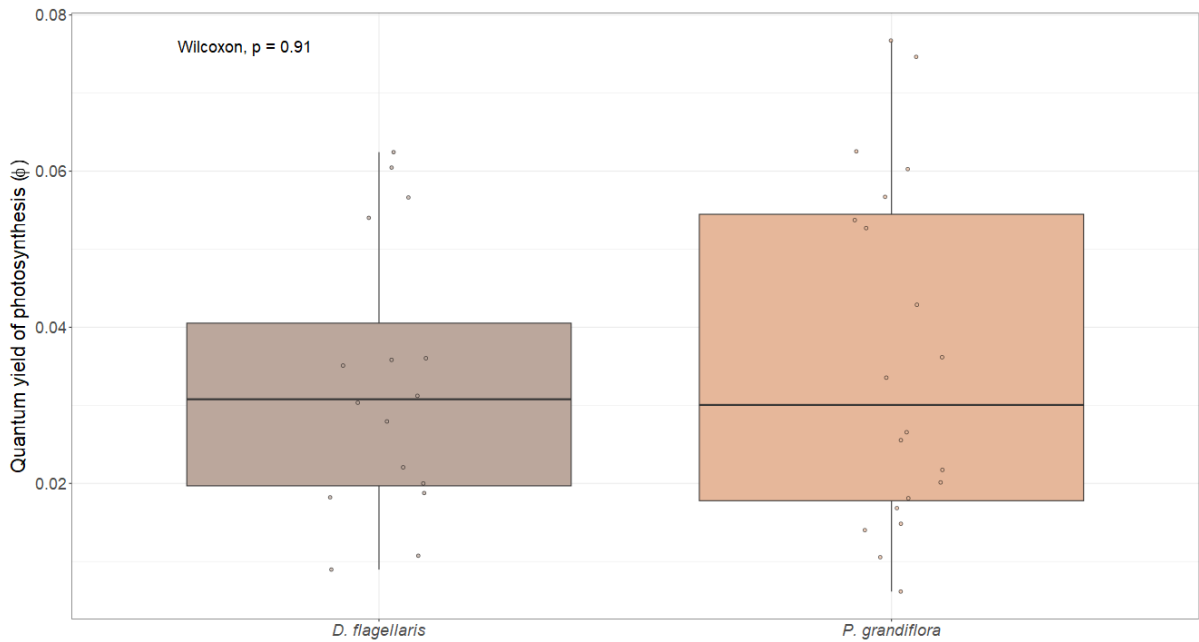


**Figure 4.5:** Boxplots showing the quantum yield estimates separated between species.

## 4.2.2 Farquhar model parameters (A/Ci)

The fitting of the A/Ci responses to the Farquhar, Caemmerer, and Berry (1980) provided several estimations of parameters for the plants studied. Despite the high range of variance in the data, as seen in Figs. 4.7 and 4.9, no significant differences between the three experimental groups or between *D. flagellaris* and *P. grandiflora* have been observed. The mean values obtained conform to previous comparable findings from the OTCs (FERRER, 2021; DAMASCENO et al., 2024). The ratio between parameters,

a recurrent value observed in plant physiology studies, has also shown no significant differences (figs A.5 and A.6).

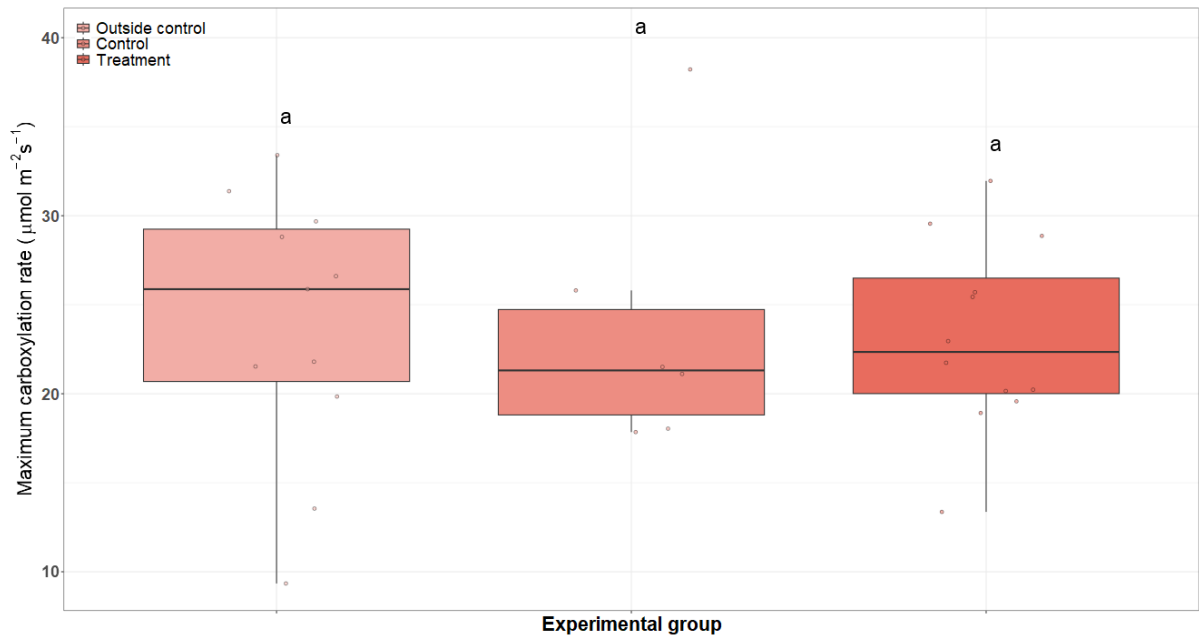


**Figure 4.6:** Boxplot showing the maximum RuBP saturated carboxylation rate ( $V_{cmax}$ ) separated between the three experimental groups of the study. The Tukey test show non-significant differences between the boxplots.

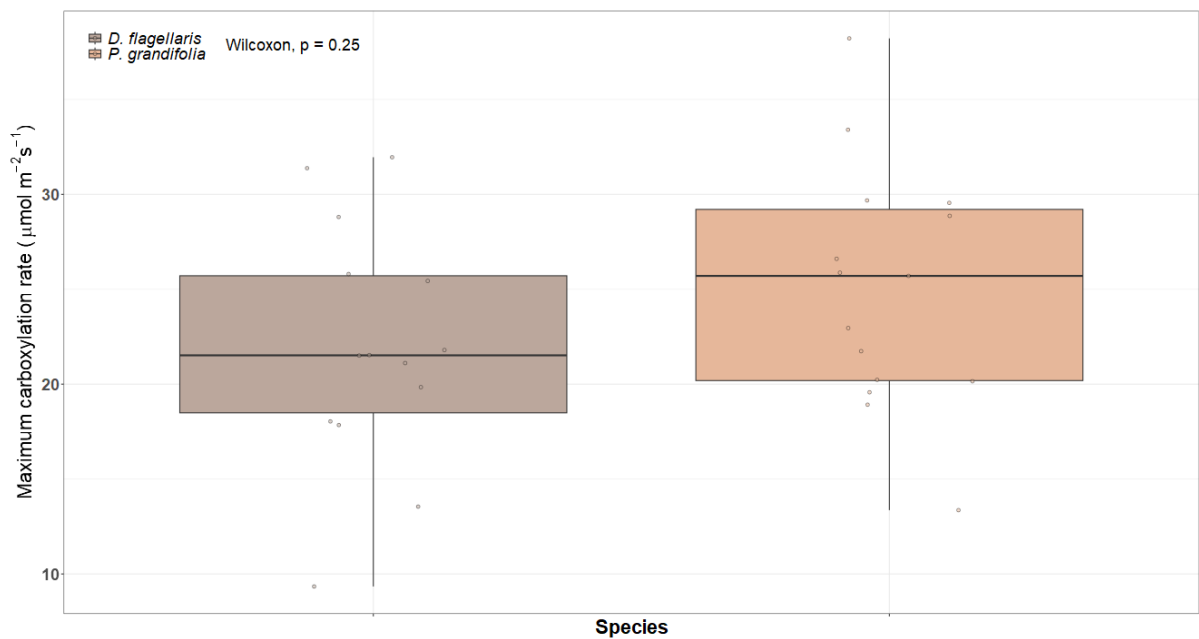


**Figure 4.7:** Boxplot showing the maximum RuBP saturated carboxylation rate ( $V_{cmax}$ ) separated between the two species used in the study. The Wilcoxon p-value show a non-significant value.

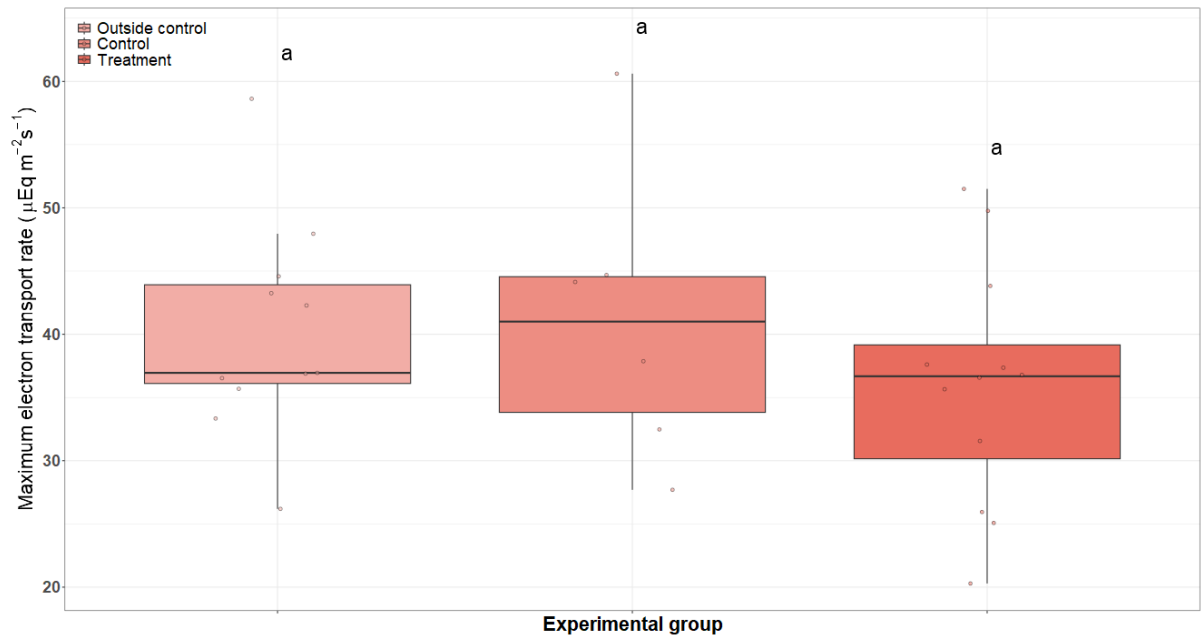


**Figure 4.8:** Boxplot showing the maximum electron transport rate ( $J_{max}$ ) separated between the three experimental groups of the study.

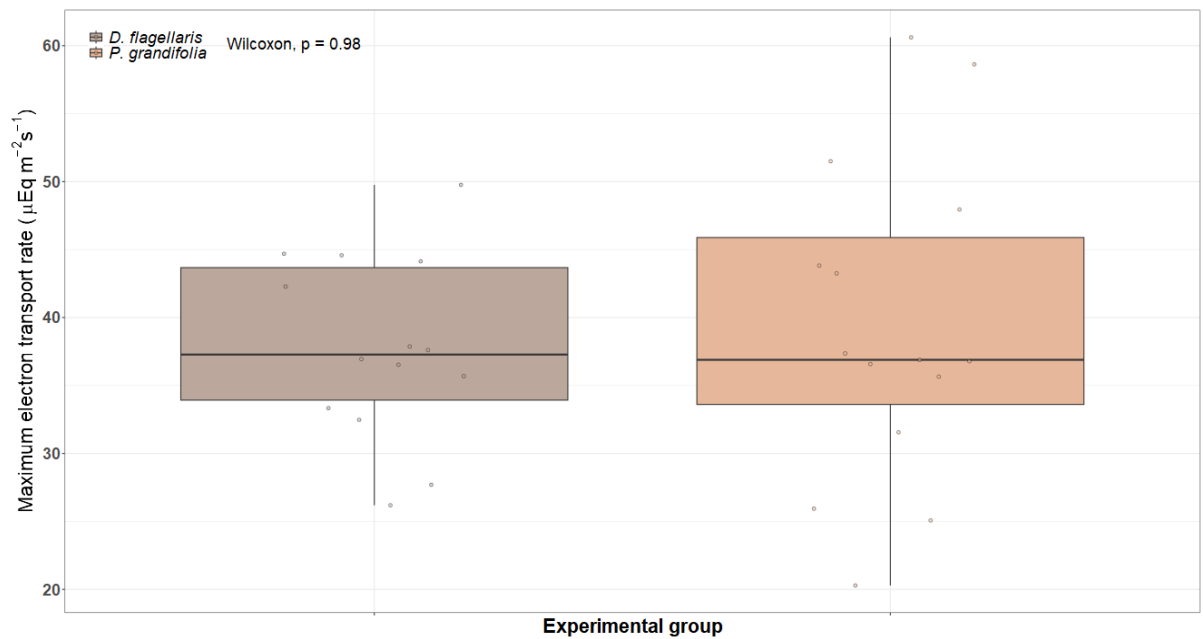


**Figure 4.9:** Boxplot showing the maximum electron transport rate ( $J_{max}$ ) separated between the two species used in the study. The Wilcoxon p-value show a non-significant value.

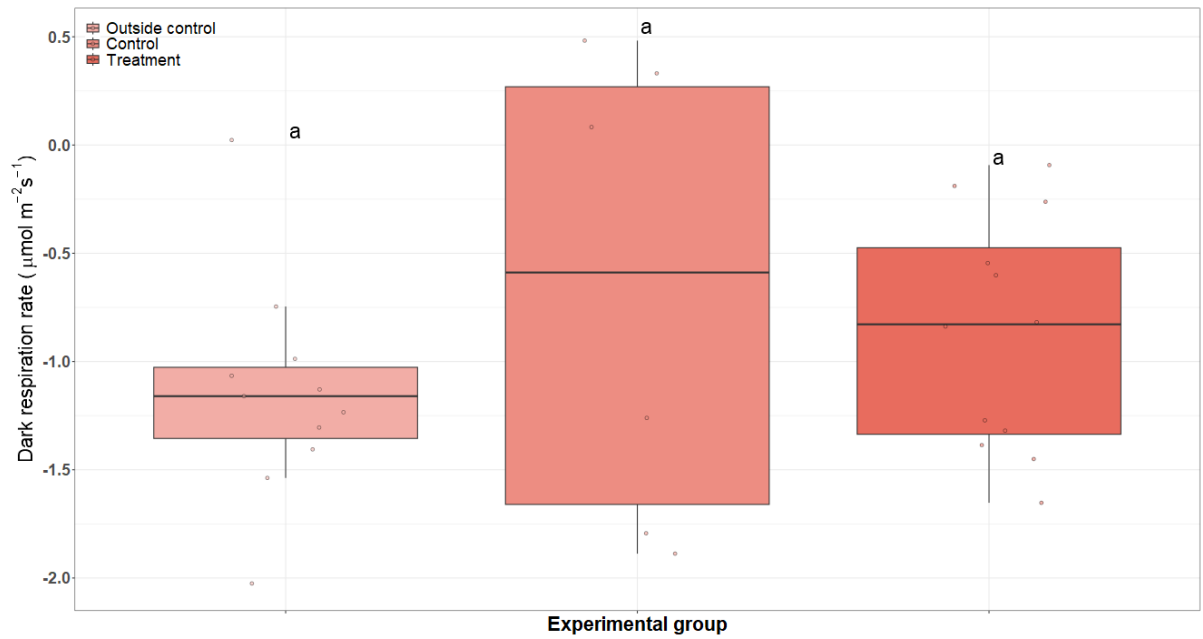


**Figure 4.10:** Boxplot showing the dark respiration rate (Rd) separated between the three experimental groups of the study.

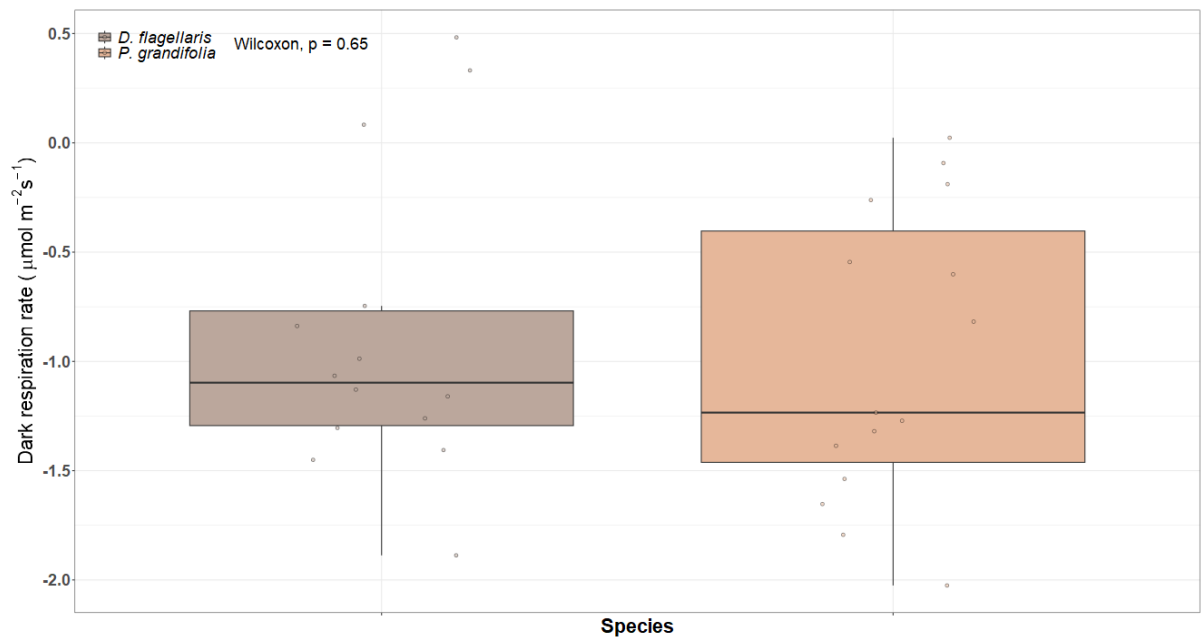


**Figure 4.11:** Boxplot showing the dark respiration rate (Rd) separated between the two species used in the study. The Wilcoxon p-value show a non-significant value.

### 4.2.3 Medlyn parameters

The fitting of the model developed by Medlyn, Duursma, Eamus, et al. (2011), as described in the Material and Methods section, was done in two different ways: with a fixed stomatal sensitivity to VPD ( $g_k$ ) value of 0.5 - the original equation of the paper - and with  $g_k$  being a variable parameter in the model. The values for both approaches presented no significant differences either between experimental groups or species, but show a high range of values. The mean  $g_1$  values are consistently higher in the fixed  $g_k$  version of the equation, and the general  $g_1$  values do not contradict the literature (LIN et al., 2015).

In the following figures (from Fig. 4.12 to Fig. 4.17) we show the jitter plots for these two approaches regarding the A/RH response curves, as the fits for A/Ci and A/Q responses were very similar. The results for these other two types of curves can be found in the appendix section. The error bars represent the standard deviation difference from the mean, which is represented by the central point in brown.

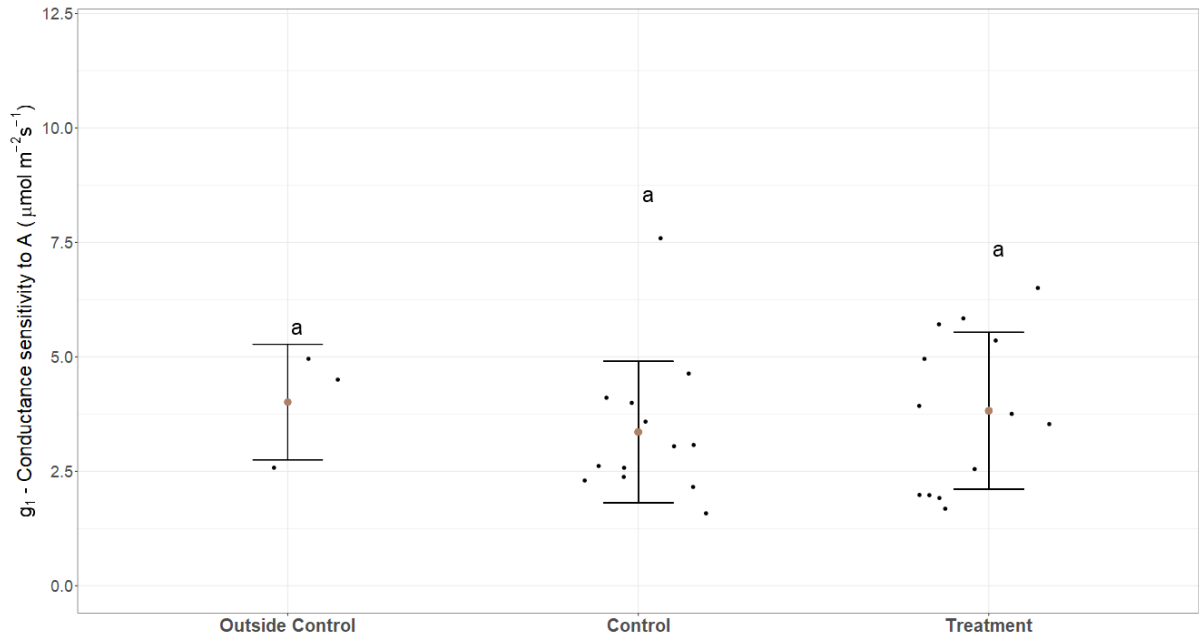


**Figure 4.12:** Jitter plot showing the  $g_1$  values obtained by fitting the variable  $g_k$  stomatal conductance model separated by experimental group. The Tukey test shows no significant differences between the boxplots.

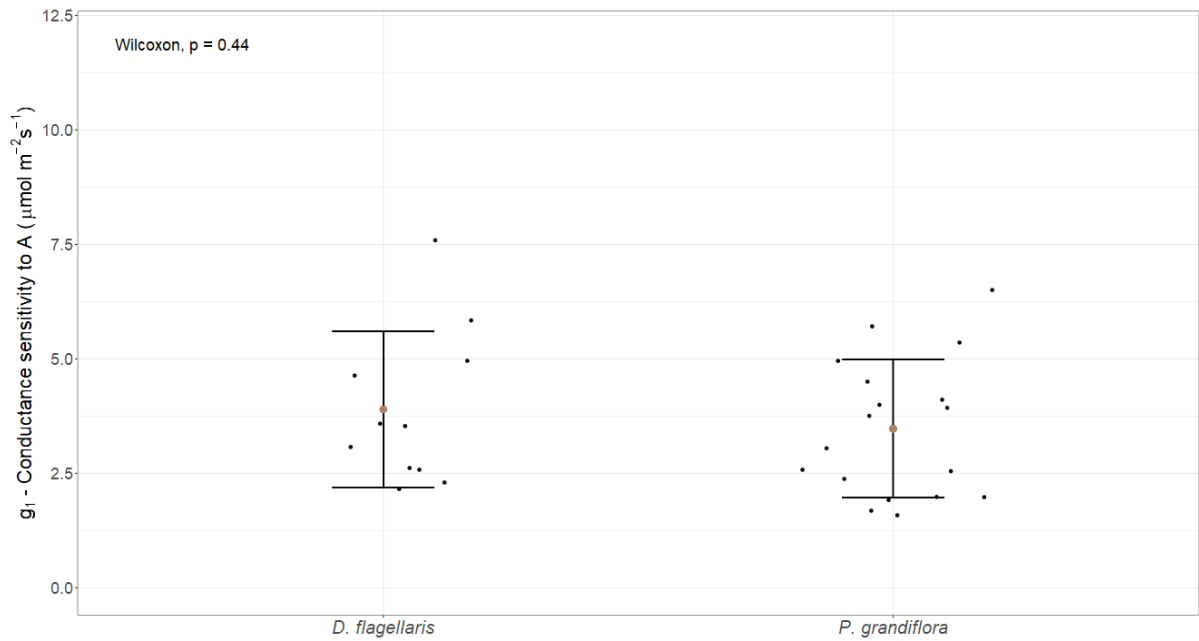


**Figure 4.13:** Jitter plot showing the  $g_1$  values obtained by fitting the variable  $g_k$  stomatal conductance model separated by species. The Tukey test shows no significant differences between the boxplots.

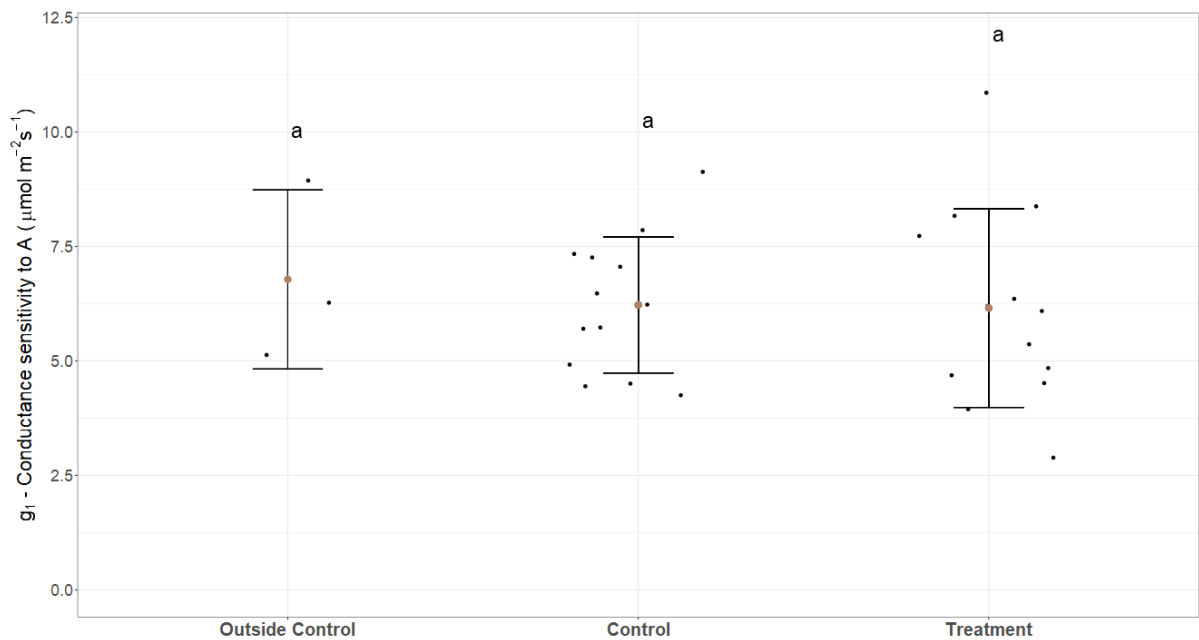


**Figure 4.14:** Jitter plot showing the  $g_1$  values obtained by fitting the fixed  $g_k$  stomatal conductance model separated by experimental group. The Tukey test shows no significant differences between the boxplots.

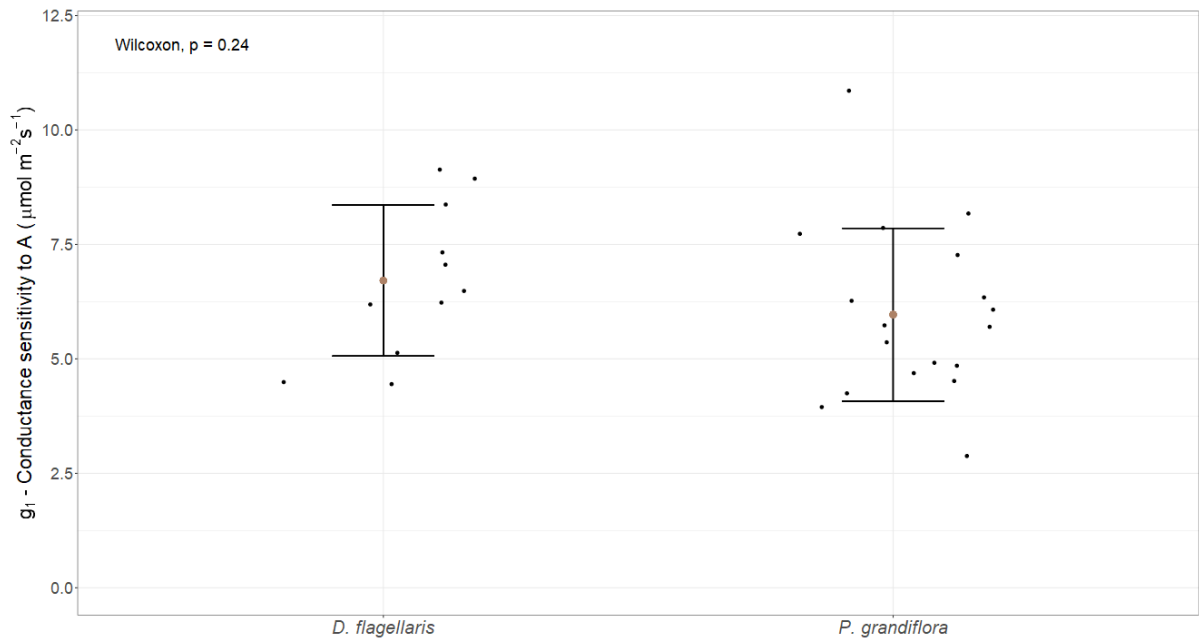


**Figure 4.15:** Jitter plot showing the  $g_1$  values obtained by fitting the fixed  $g_k$  stomatal conductance model separated by species. The Wilcoxon p-value shows no significant differences between the boxplots.

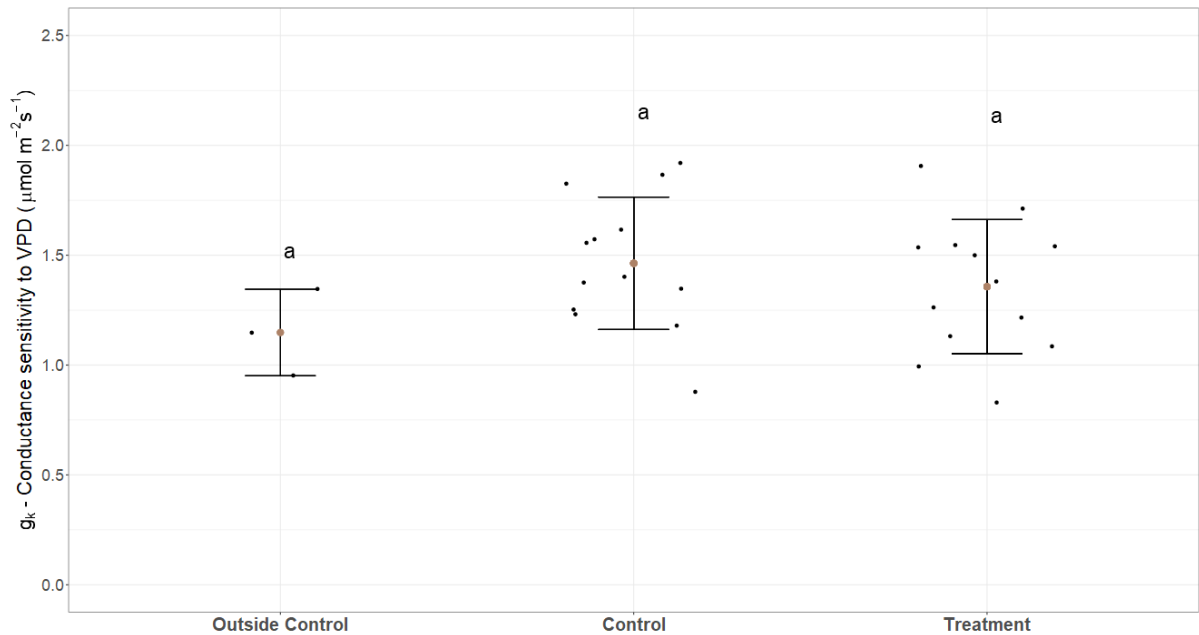


**Figure 4.16:** Jitter plot showing the  $g_k$  values obtained by fitting the variable  $g_k$  stomatal conductance model separated by experimental group. The Tukey test shows no significant differences between the boxplots.

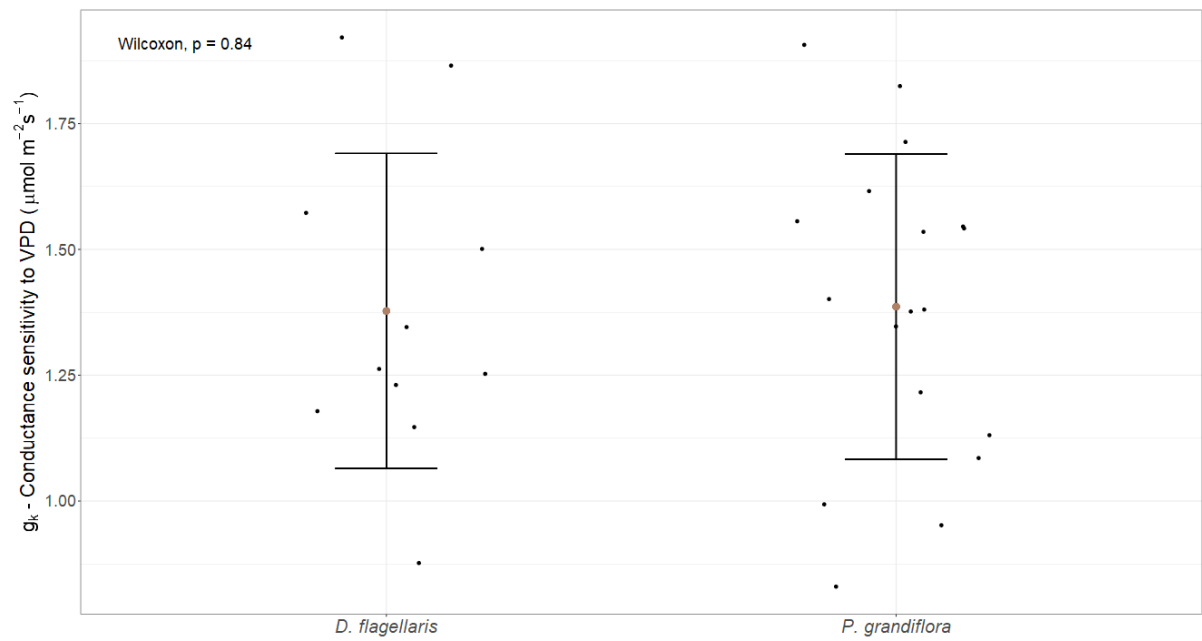


**Figure 4.17:** Jitter plot showing the  $g_k$  values obtained by fitting the variable  $g_k$  stomatal conductance model separated by species. The Wilcoxon p-value shows no significant differences between the boxplots.

#### 4.2.4 Curve fits

Examples of the curve fittings and measured values of the data obtained during the field campaign are available in the appendix (Figs. A.7 to A.11). Generally, the fittings behave as expected for each model, with one particular observation. The initial inclination of the fitting for A/Q response was significantly steeper than what is usually reported in the literature (SOUZA et al., 2010), which was assumed to be a consequence of the behavior of species adapted to the light limitations of the understory, where efficiently utilizing scarce sunflecks can be a compensatory strategy.

### 4.3 Stomatal conductance measurements

The gas exchange measurements of stomatal conductance show a significant difference between *D. flagellaris* and *P. grandiflora* ( $p = 0.0052$ , Fig. 4.19). Between the experimental groups, no significant differences were observed (Fig. 4.18), which was expected based on the literature (ALENCAR et al., 2024). When splitting the data by the relative humidity intervals (Fig. 4.20), there is a clear decrease in conductance for the highest humidity values, which can be explained by the low air VPD in the chamber during these conditions.

The measured values of stomatal conductance, when compared between experimental groups for the light response and CO<sub>2</sub> response curves, present an increase in the treatment groups (Figs. A.1 and A.3). However, this type of comparison is subjected to several biases, such as size and individual responses. For this reason, the comparison here is mainly focused on the model parameters estimated from these measurements and the A/RH response measurements, leaving the other plots for the appendix section.

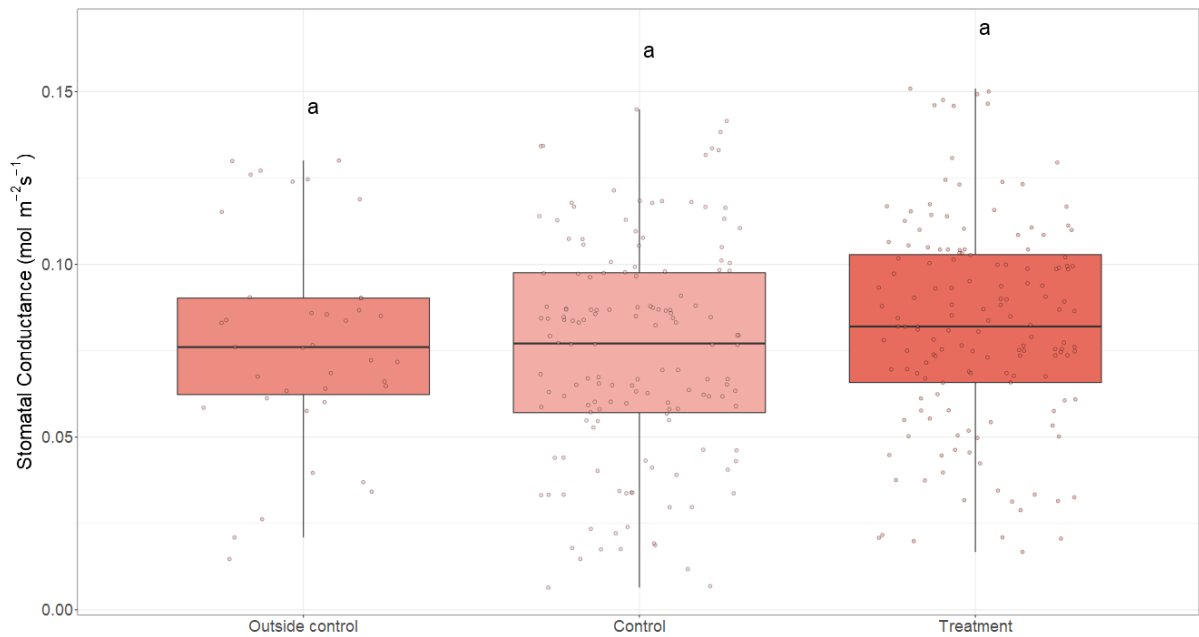


**Figure 4.18:** Stomatal conductance value measured during A/RH response curves. The values are separated according to each experimental group that the data corresponds to.

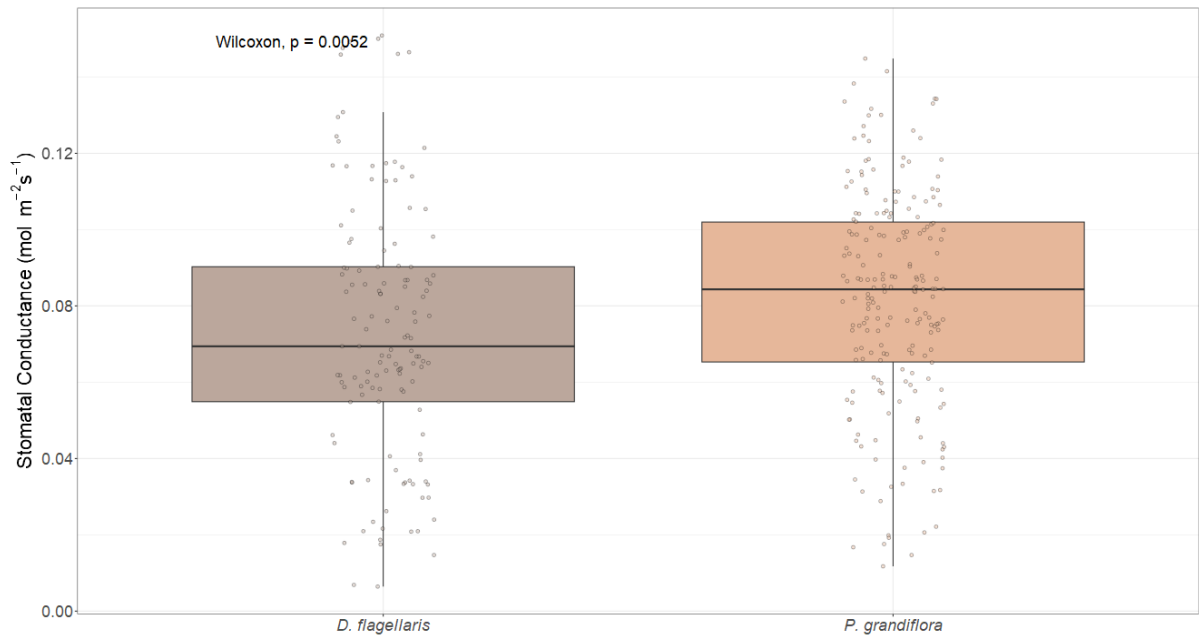


**Figure 4.19:** Stomatal conductance values measured during A/RH response curves. The values are separated according to the species that the data corresponds to, with the Wilcoxon p-value indicating a significant difference between the boxplots.

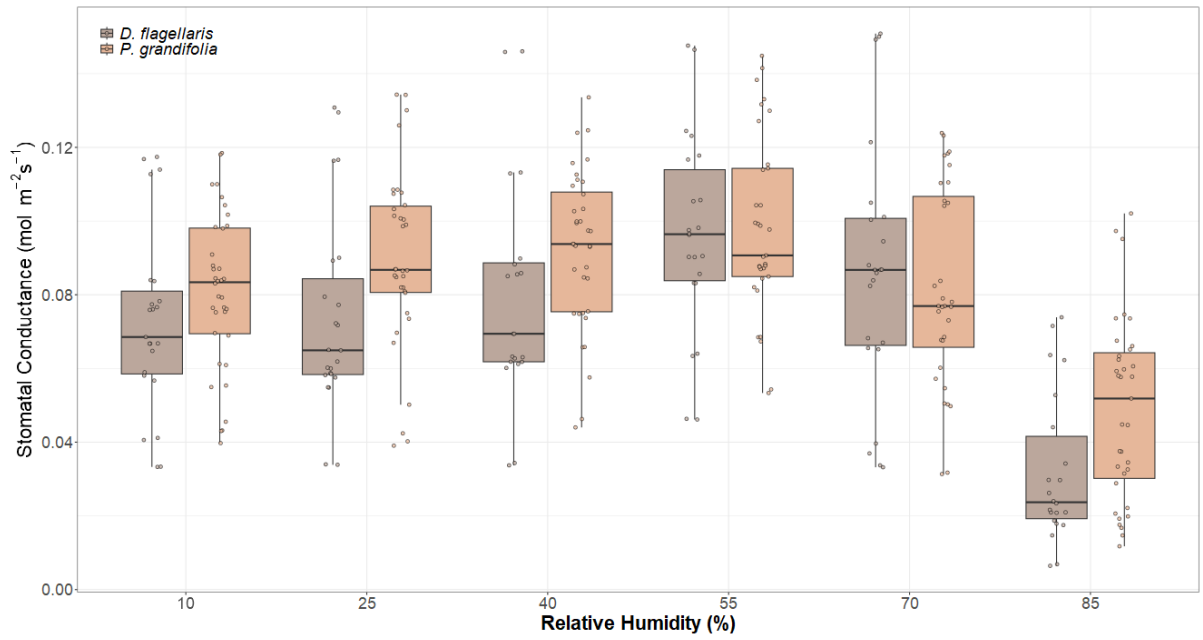


**Figure 4.20:** Stomatal conductance values measured during A/RH response curves separated by relative humidity interval in the x axis. The values are separated in boxplots according to the species that the data corresponds to.

## 4.4 Big-leaf model

### 4.4.1 Estimated results without the inclusion of leaf area

The estimations obtained using the big-leaf model approach described in section 3.9 produced results for three variables: net  $\text{CO}_2$  assimilation, stomatal conductance and transpiration. As the plots distributions were similar between the variables, in this section are presented only the transpiration figures (Figs. 4.21, 4.22 and 4.23), while the rest of the results can be found in the appendix (figs A.15 to A.19). In general, the approach showed a difference in the results for each species, but no significant changes among experimental groups. For the net  $\text{CO}_2$  assimilation and stomatal conductance values, the resulting boxplots were rather similar, only showing a slight increase for the treatment group that can be attributed to the difference in leaf area (Figs. A.15 and A.16). In this subsection, the plots do not consider individual leaf area, showing the summed result for the simulated period, with each dot representing one individual.

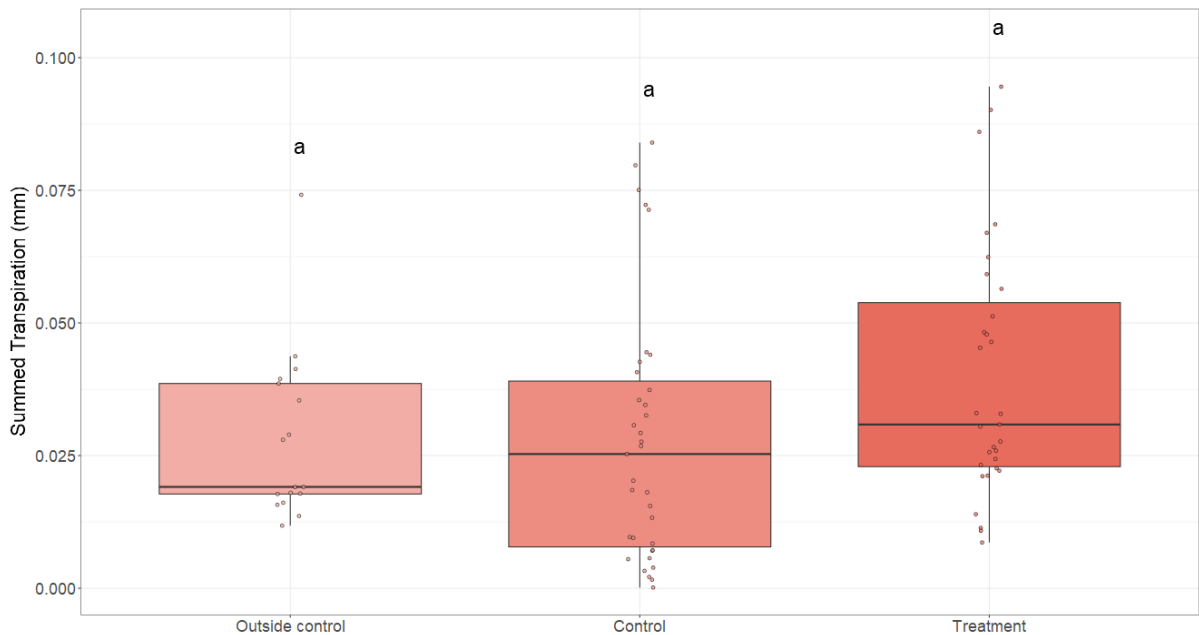


**Figure 4.21:** Boxplots showing the transpiration values estimated by the big leaf model using the full Medlyn model parameters separated by experimental group. The Tukey test indicates a significant increase in the treatment group in relation to the other two.

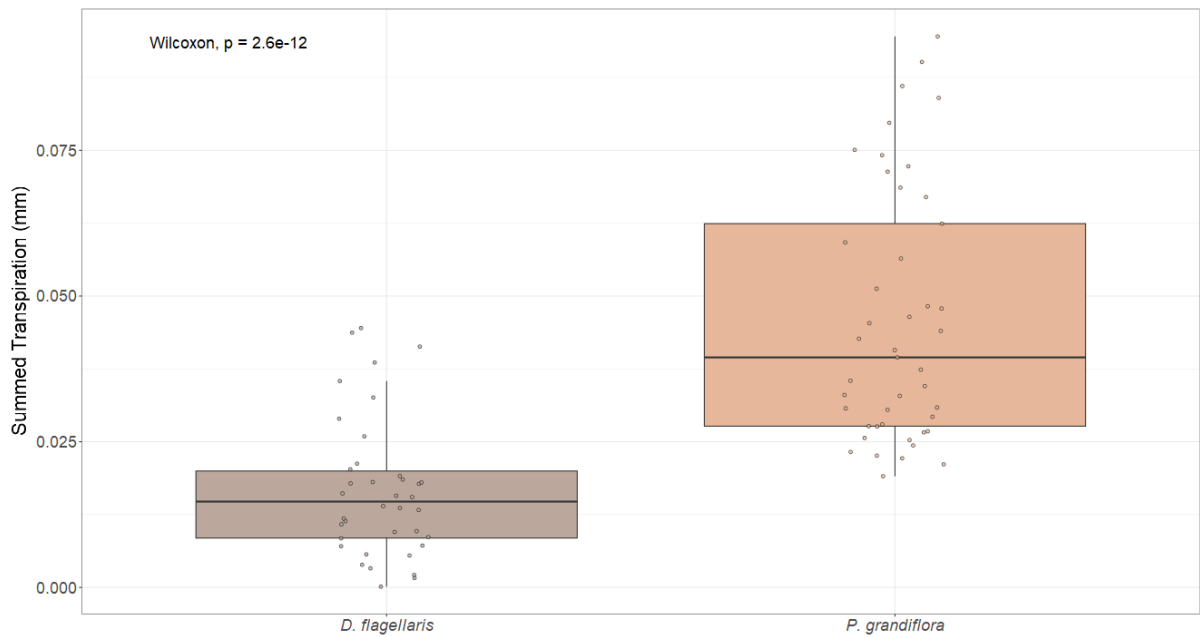


**Figure 4.22:** Boxplots showing the transpiration values estimated by the big leaf model using the full Medlyn model parameters separated by species. The Wilcoxon p-value indicates a significant difference between the two boxplots.

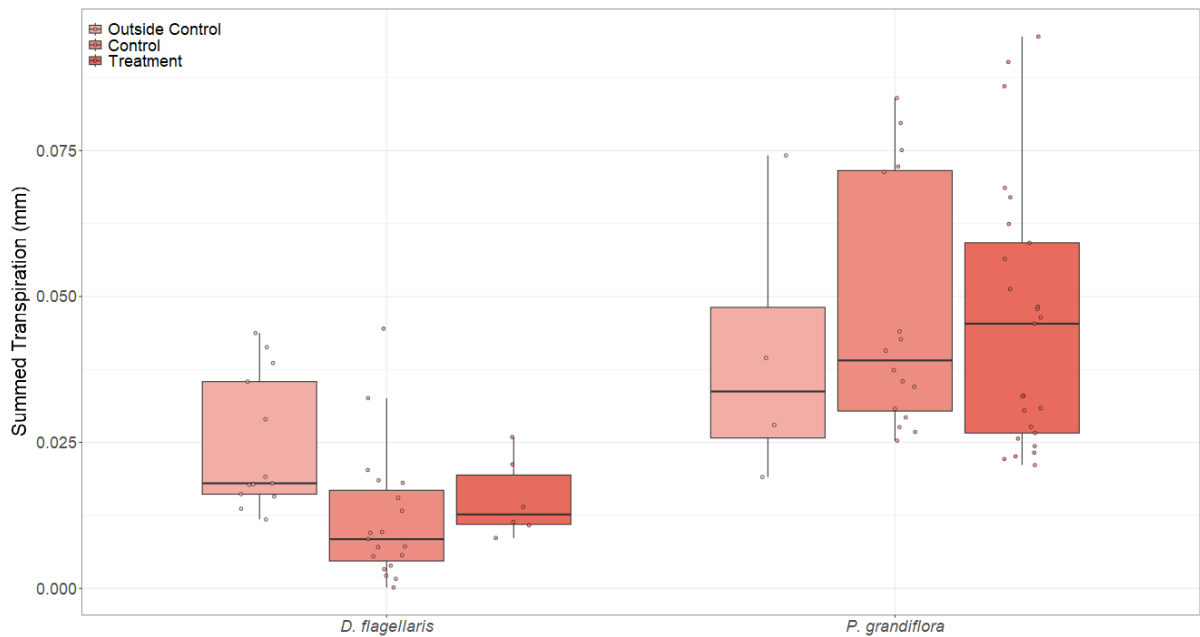


**Figure 4.23:** Boxplots showing the transpiration values estimated by the big leaf model using the full Medlyn model parameters separated by species and experimental groups. The boxplots show no consistent differences in experimental groups that are present for both species.

#### 4.4.2 Estimated results including leaf area

When leaf area values for each individual were included in the evaluation, the differences between species became even more significant (fig 4.25), impacting the results of the experimental groups plot (Fig. 4.24). Even so, when analyzing the experimental groups and species separated, it is still not possible to observe a consistent difference

caused by the treatment on both species (Fig. 4.26), a result that was also observed when comparing the leaf area values directly (Figs. A.12 to A.14), where the difference can only be perceived for *P. grandiflora*. The leaf area measurements are presented in the appendix. In this subsection, the summed transpiration found is multiplied by individual leaf area, providing an estimation in grams of water for the simulated period.

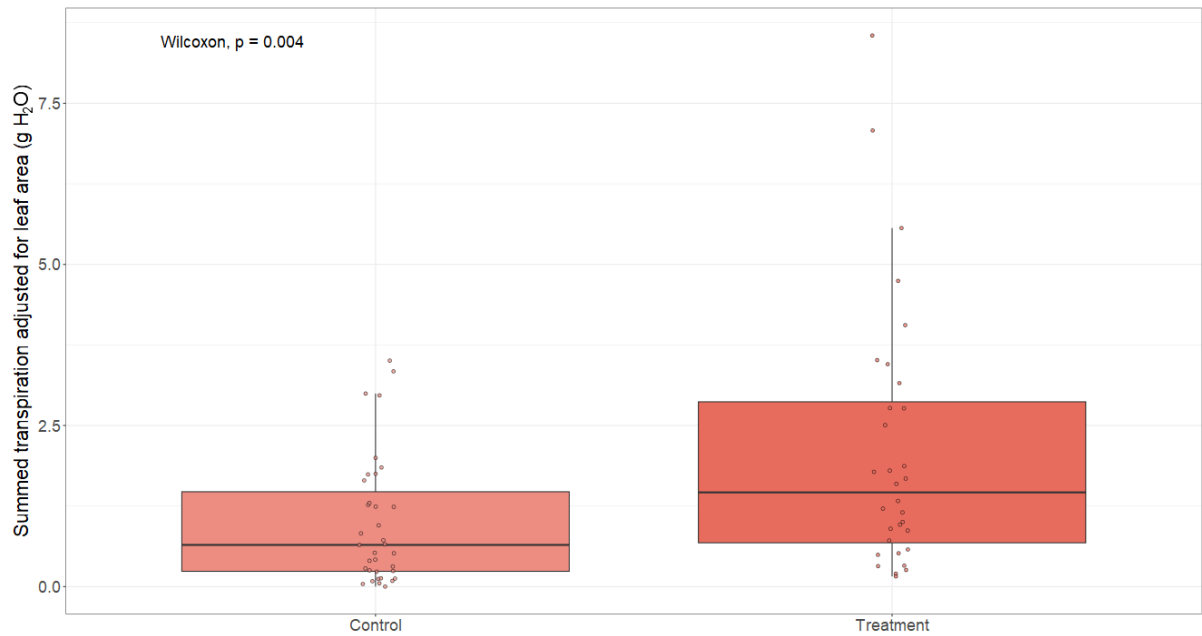


**Figure 4.24:** Boxplots showing the transpiration values adjusted by leaf area that were estimated by the big leaf model using the full Medlyn model parameters separated by experimental group. The Tukey test indicates no significant differences between the groups.

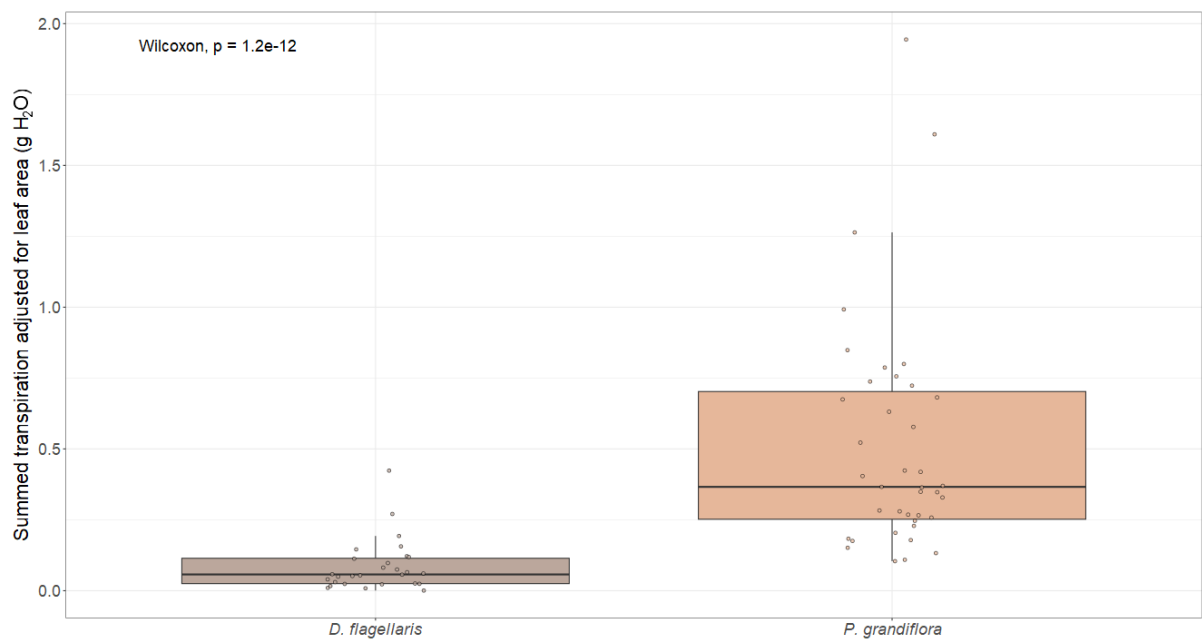


**Figure 4.25:** Boxplots showing the transpiration values adjusted by leaf area that were estimated by the big leaf model using the full Medlyn model parameters separated by species. The Wilcoxon p-value indicates a significant difference between the two boxplots.

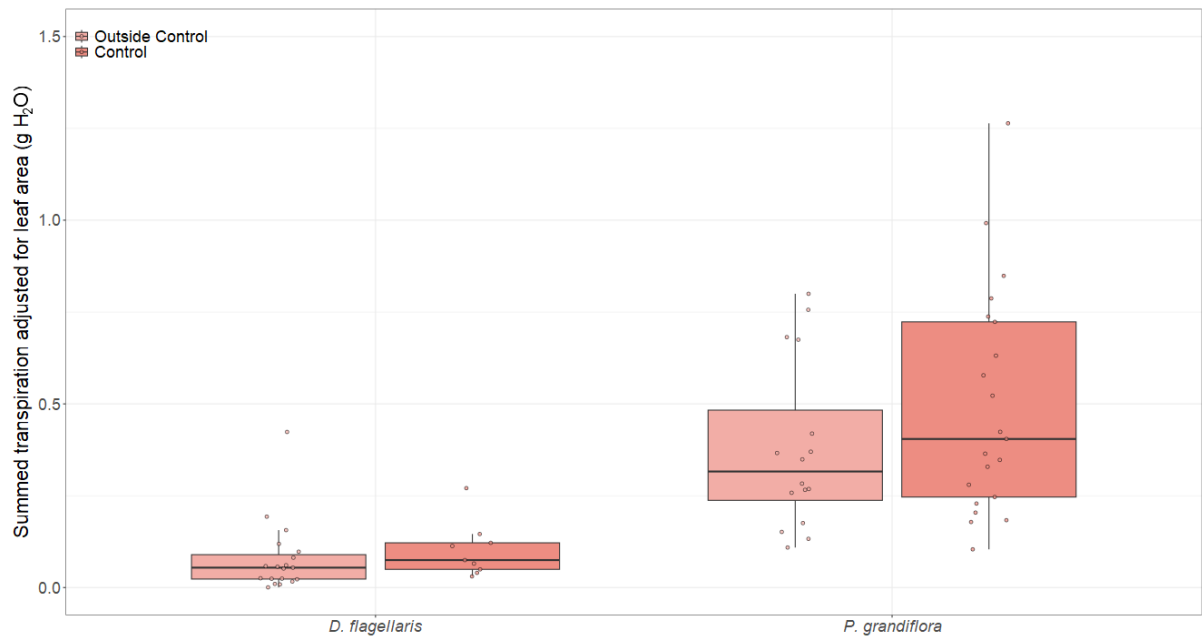


**Figure 4.26:** Boxplots showing the transpiration values adjusted by leaf area that were estimated by the big leaf model using the full Medlyn model parameters separated by species and experimental groups. The boxplots show no consistent differences in experimental groups present for both species.

## Discussion

The results obtained present, in general, few differences between experimental groups, indicating that the CO<sub>2</sub> increase created by the experiment does not alter most of the estimated physiological parameters of the two species analyzed, at least for a short term period, a result that agrees with the majority of the literature in this regard (THOMAS; DELUCIA, 2000; XU; JIANG; JIA, et al., 2016; ALENCAR et al., 2024). The main differences observed are on some of the aspects regarding the stomatal conductance of *D. flagellaris* and *P. grandiflora*, as the measured values obtained with the IRGA curves present a difference (Fig. 4.19), which was also the case with the upscaled summed values obtained via the big-leaf model approach (Fig. 4.25). Even so, the physiological parameters  $g_1$  and  $g_k$  from Medlyn, Duursma, Eamus, et al. (2011) equation, in contrast with the stomatal conductance values, do not present significant changes.

Regarding the Farquhar model parameters  $V_{cmax}$  and  $J_{max}$ , the values fluctuate around previous reports for the OTC experiment (FERRER, 2021; DAMASCENO et al., 2024). Although these previous studies have found differences between experimental groups, the species used were rather different and, for Ferrer (2021), which only found differences for  $J_{max}/V_{cmax}$  ratios, also fertilized with phosphorus. Overall, the  $J_{max}/V_{cmax}$  ratio was similar, showing no clear differences between experimental groups or species. Data from canopy tropical species, however, present higher values than the OTC estimations, providing a potentially interesting comparison between these parameters when inputted in the big-leaf model or a two-leaf model, since shaded can present lower parameter values (HERNÁNDEZ; WINTER; SLOT, 2021).

Although few significant differences between the groups have been observed, there is a high variance in values within each variable, a pattern also evident when the data is separated by species. This high variance suggests that both species present a big variability regarding the possible parameter values. This finding could indicate a high resilience of the community to changes, as both populations seem to be able to physiologically sustain several environmental conditions in relation to the physiological

parameter values. It would be beneficial to investigate, at the experimental site, whether the wide range of values derived from low sampling of leaves from each individual or not.

Aside from the variance in values, it is important to notice, as a potential difference that could lead to changes in the community, the observed differences in stomatal conductance and transpiration results indicate a difference in water use between both species, which is even more accentuated when taking in consideration individual leaf area (Figs. 4.25 and A.16). Since both dominant species exhibit significant variability in parameters and potentially different water use strategies, the results suggest a potential for community shifts in response to small environmental changes, although more data is necessary for such affirmation.

The seasonal effect of climate on the responses measured by the present study could not be evaluated, as only one field campaign was successfully conducted. This possible effect, reported in the literature for photosynthesis parameters for decades (MEDLYN; LOUSTAU; DELZON, 2002), may induce some plasticity in relation to parameters such as  $g_1$ ,  $g_k$  and  $V_{cmax}$  when considering the high variability of parameter values found, therefore being an important factor to be considered in future measurements of similar data at the experimental site.

Previous findings in the present OTC experiment, as described in Damasceno et al. (2024), show a significant difference between the total leaf area of experimental groups (Fig. A.12). This result aligns with previous publications on the topic, though these studies pertain to different environments (ZHAN et al., 2022; MCCARTHY et al., 2006), indicating short-term leaf plasticity in response to elevated  $CO_2$ . Even so, it is unclear whether this response would be maintained and, in relation to water flux, remain unaffected by other factors in a longer time scale, as stomatal density, for example, has been reported to decrease in such conditions (XU; JIANG; JIA, et al., 2016). It is also not equally evident for both species, when plotted separately (Fig. A.14).

Scaling up the data temporally and spatially elucidated the differences in stomatal conductance and transpiration presented by the model, showing a big difference in values between species (Fig. 4.25), but no significant changes between experimental groups (Figs. 4.21 and 4.26). This result, when analyzed in conjunction with the reasonable parameter values estimated from field data (in comparison with Lin et al. (2015)), supports the assumption that the mathematical model of Medlyn, Duursma, Eamus, et al. (2011) here used can reproduce, at least for the purposes of this

study, the dynamics of amazonian understory species in relation to the plant-atmosphere water flux, since both approaches yielded similar results.

Still on the model of stomatal conductance, it is also important to elucidate what can be interpreted from the mean values of  $g_1$  and  $g_k$ . The mean  $g_1$  values obtained are consistently higher than those reported in the literature for tropical rainforest trees (LIN et al., 2015). This is a reasonable estimate, as the abiotic factors of the understory support strategies less conservative in water use, that would present a higher  $g_1$ . Regarding  $g_k$ , the variable version of the model provided values always higher than the default  $0.5 \text{ kPa}^{-1}$  of the fixed model. Higher values for the parameter indicate a lower magnitude in the response of stomatal conductance to atmospherical VPD, which supports the hypothesis for species acclimated to shaded environments such as the understory stratum. (LIN et al., 2015; LAMOUR et al., 2022), where the consistently high relative humidity reduces the need for stomatal closure to conserve water.

The expected reduction in stomatal conductance in high  $\text{CO}_2$  concentrations (MORISON, 1998), although not observed between experimental groups, was still present in the individual gas exchange  $A/C_i$  curves (Fig. A.8), reinforcing the validity of the measurements and the response of the two species. On the other hand, the decrease of stomatal conductance in  $A/RH$  curves at the highest RH values was unexpected but can be interpreted as a response to the low negative water pressure between the air in the chamber and the leaf tissue (OTTOSEN; MORTENSEN; GISLERØD, 2002).

With the collected and estimated data presented here, we put forward the hypothesis that, given the high intraspecific diversity observed in the estimates and the differences in stomatal conductance and transpiration (Figs. 4.19 and 4.20), community shifts in response to climate change are plausible in this system, even though the  $g_1$  and  $g_k$  means did not show a clear difference in water use strategies as seen in the stomatal conductance values. However, it is not possible to assume the direction of these possible shifts, as a study conducted continuously over a longer time scale would be necessary to sustain more concrete assumptions. Ideally, more species from the understory community should be studied in order to determine if there is a general response of the majority of dominant species and the possible differences between them, as this could be key to understanding potential community shifts in the future.

# Conclusion

In order to conclude the ideas presented in this project, it is important to first elucidate the uniqueness of one aspect of the ecosystem studied in the AmazonFACE program compared to previous FACE projects: its hyperdiversity. A major part of the uncertainty and inconclusiveness of these results come from the fact that studying two species from a hyperdiverse ecosystem will not provide enough insights into its general responses; instead providing an starting point for discussion, as well as a characterization of the species and, for this case, an evaluation of the physiological models' performances under such conditions.

The findings presented here clarify how physiological aspects of two dominant plant species from the Amazon understory respond, on a short time scale, to elevated CO<sub>2</sub> concentrations. The high intraspecific diversity of parameter values elucidates the potential plasticity of the plant community to these changes, a result that has not been demonstrated for the region until now and agrees with what is suggested in the literature (XU; JIANG; JIA, et al., 2016), which needs to be explored further by comparing leaf flushes and sustained long-term effects. When combined with the differences in water use of the species presented in the discussion, these results raise the question of whether the possibility of community shifts being observed in the next decades in relation to climate change effects on the water cycle, that may act as an inflection point for the community diversity.

In addition to the general community aspects interpreted from the results, the characterization of both species, in relation to what is possible to infer with the IRGA data, is also a significant stepping stone for the development of the knowledge of the central Amazon rainforest hyperdiverse ecosystems, as most of the species composing the community are understudied due to numerous tropical taxonomic shortfalls (BARLOW et al., 2018; ALENCAR et al., 2024).

The data presented clearly indicate that further research in the AmazonFACE program is necessary to determine if this variance is consistent across a broader range of species within the community, with a larger number of measurements on individual subjects during a longer time scale. Such research would enable the formulation of more concrete implications for the future of the ecosystem. The results presented thus far

serve as a starting point for this discussion, yet are insufficient to conclude it, leaving the question: where will 10 more years of experimentation in AmazonFACE lead our knowledge?

# References

AINSWORTH, E. A.; LONG, S. P. What have we learned from 15 years of free-air CO<sub>2</sub> enrichment (FACE)? A meta-analytic review of the responses of photosynthesis, canopy properties and plant production to rising CO<sub>2</sub>. **New Phytologist**, v. 165, p. 351–372, 2 Feb. 2005. ISSN 0028646X. DOI: 10.1111/j.1469-8137.2004.01224.x.

ALENCAR, A. S. de et al. Twenty-five years of Open-Top Chambers in tropical environments: where, how, and what are we looking at regarding flora response to climate change? **Planta**, Springer Science and Business Media Deutschland GmbH, v. 259, 4 Apr. 2024. ISSN 14322048. DOI: 10.1007/s00425-024-04356-8.

AMAZONFACE. **AmazonFACE home page**. 2024. Available from: <<https://amazonface.unicamp.br>>. Visited on: 20 May 2024.

ARNONE, J. A.; KÖRNER, C. Influence of elevated CO<sub>2</sub> on canopy development and red:far-red ratios in two-storied stands of *Ricinus communis*. **Oecologia**, Springer-Verlag, v. 94, p. 510–515, 4 Dec. 1993. ISSN 00298549. DOI: 10.1007/BF00566966.

BADER, M. Y. et al. Simulating climate change in situ in a tropical rainforest understorey using active air warming and CO<sub>2</sub> addition. **Ecology and Evolution**, John Wiley and Sons Ltd, v. 12, 1 Jan. 2022. ISSN 20457758. DOI: 10.1002/ece3.8406.

BARLOW, J. et al. The future of hyperdiverse tropical ecosystems. **Nature**, Nature Publishing Group, v. 559, p. 517–526, 7715 July 2018. ISSN 14764687. DOI: 10.1038/s41586-018-0301-1.

BAZZAZ, F. A. The response of natural ecosystems to the rising global CO<sub>2</sub> levels. **Annual Review of Ecology, Evolution, and Systematics**, v. 21, p. 167–196, 1990. DOI: 10.1146/ANNUREV.ES.21.110190.001123.

BERNACCHI, C. J. et al. Improved temperature response functions for models of Rubisco-limited photosynthesis. **Global Change Biology**, John Wiley and Sons Inc, v. 21, p. 253–259, 3 Feb. 2001. ISSN 13652486. DOI: 10.1111/J.1365-3040.2001.00668.X.

CHIANUCCI, F.; MACEK, M. **hemispheR: Processing Hemispherical Canopy Images**. 2024. Available from: <<https://CRAN.R-project.org/package=hemispheR>>. Visited on: 10 June 2024.

DAMASCENO, A. R. et al. In situ short-term responses of Amazonian understory plants to elevated CO<sub>2</sub>. **Plant Cell and Environment**, John Wiley and Sons Inc, v. 47, p. 1865–1876, 5 May 2024. ISSN 13653040. DOI: 10.1111/pce.14842.

FARQUHAR, G. D.; CAEMMERER, S. V.; BERRY, J. A. A Biochemical Model of Photosynthetic CO<sub>2</sub> Assimilation in Leaves of C<sub>3</sub> Species. **Planta**, v. 149, p. 78–90, 1980.

FERRER, V. R. **Aumento da concentração de CO<sub>2</sub> e adição de fósforo nos fluxos de carbono e energia do processo fotossintético de plântulas de *Inga edulis* Mart. no sub-bosque da Amazônia Central**. [S.l.: s.n.], 2021. Available from: <[https://repositorio.inpa.gov.br/bitstream/1/37916/1/DISSERTA%C3%87%C3%830\\_Vanessa%20Ferrer\\_final.pdf](https://repositorio.inpa.gov.br/bitstream/1/37916/1/DISSERTA%C3%87%C3%830_Vanessa%20Ferrer_final.pdf)>.

FLEISCHER, K. et al. Amazon forest response to CO<sub>2</sub> fertilization dependent on plant phosphorus acquisition. **Nature Geoscience**, Nature Publishing Group, v. 12, p. 736–741, 9 Sept. 2019. ISSN 17520908. DOI: 10.1038/s41561-019-0404-9.

GISSI, E. et al. A review of the combined effects of climate change and other local human stressors on the marine environment. **Science of the Total Environment**, Elsevier B.V., v. 755, Feb. 2021. ISSN 18791026. DOI: 10.1016/j.scitotenv.2020.142564.

GU, L. et al. Reliable estimation of biochemical parameters from C<sub>3</sub> leaf photosynthesis-intercellular carbon dioxide response curves. **Plant, Cell and Environment**, v. 33, p. 1852–1874, 11 Nov. 2010. ISSN 01407791. DOI: 10.1111/j.1365-3040.2010.02192.x.

HE, J. S.; BAZZAZ, F. A.; SCHMID, B. Interactive effects of diversity, nutrients and elevated CO<sub>2</sub> on experimental plant communities. **Oikos**, v. 97, p. 337–348, 3 2002. ISSN 00301299. DOI: 10.1034/j.1600-0706.2002.970304.x.

HERNÁNDEZ, G. G.; WINTER, K.; SLOT, M. Similar temperature dependence of photosynthetic parameters in sun and shade leaves of three tropical tree species. **Tree**

**Physiology**, Oxford University Press, v. 40, p. 637–651, 5 2021. ISSN 17584469. DOI: 10.1093/TREEPHYS/TPAA015.

HUBAU, W. et al. The persistence of carbon in the African forest understory. **Nature Plants**, Palgrave Macmillan Ltd., v. 5, p. 133–140, 2 Feb. 2019. ISSN 20550278. DOI: 10.1038/s41477-018-0316-5.

IPCC. **IPCC, 2023: Climate Change 2023: Synthesis Report. Contribution of Working Groups I, II and III to the Sixth Assessment Report of the Intergovernmental Panel on Climate Change [Core Writing Team, H. Lee and J. Romero (eds.)]. IPCC, Geneva, Switzerland.** Ed. by Paola Arias. [S.l.: s.n.], July 2023. DOI: 10.59327/IPCC/AR6-9789291691647. Available from: <<https://www.ipcc.ch/report/ar6/syr/>>.

JIANG, M. et al. The fate of carbon in a mature forest under carbon dioxide enrichment. **Nature**, Nature Research, v. 580, p. 227–231, 7802 Apr. 2020. ISSN 14764687. DOI: 10.1038/s41586-020-2128-9.

JIMÉNEZ-RODRÍGUEZ, C. D. et al. Contribution of understory evaporation in a tropical wet forest during the dry season. **Hydrology and Earth System Sciences**, Copernicus GmbH, v. 24, p. 2179–2206, 4 Apr. 2020. ISSN 16077938. DOI: 10.5194/hess-24-2179-2020.

KAPPEN, L.; ANDRESEN, G.; LOSCH, R. In situ Observations of Stomatal Movements 1. **Journal of Experimental Botany**, v. 38, p. 126–141, 186 1987. Available from: <<http://jxb.oxfordjournals.org/>>.

LAMOUR, J. et al. An improved representation of the relationship between photosynthesis and stomatal conductance leads to more stable estimation of conductance parameters and improves the goodness-of-fit across diverse data sets. **Global Change Biology**, John Wiley and Sons Inc, v. 28, p. 3537–3556, 11 June 2022. ISSN 13652486. DOI: 10.1111/gcb.16103.

LAPOLA, D. M.; NORBY, R. J. Assessing the effects of increased atmospheric CO<sub>2</sub> on the ecology and resilience of the Amazon forest. **AmazonFACE research plan**, 2014.

LEUNING, R. et al. Leaf nitrogen, photosynthesis, conductance and transpiration: scaling from leaves to canopies. **Plant, Cell & Environment**, v. 18, p. 1183–1200, 10 1995. ISSN 13653040. DOI: 10.1111/j.1365-3040.1995.tb00628.x.

LIMA, L. S. et al. Feedbacks between deforestation, climate, and hydrology in the Southwestern Amazon: Implications for the provision of ecosystem services. **Landscape Ecology**, v. 29, p. 261–274, 2 Feb. 2014. ISSN 09212973. DOI: 10.1007/s10980-013-9962-1.

LIN, Y. S. et al. Optimal stomatal behaviour around the world. **Nature Climate Change**, Nature Publishing Group, v. 5, p. 459–464, 5 May 2015. ISSN 17586798. DOI: 10.1038/nclimate2550.

MACHÁČOVÁ, K. Open top chamber and free air CO<sub>2</sub> enrichment - approaches to investigate tree responses to elevated CO<sub>2</sub>. **iForest – Biogeosciences and Forestry**, v. 3, p. 102–105, 2010. DOI: 10.1111/j.1469-8137.2004. Available from: <<http://www.sisef.it/iforest/>>.

MAIER, C. A. et al. The response of coarse root biomass to long-term CO<sub>2</sub> enrichment and nitrogen application in a maturing *Pinus taeda* stand with a large broadleaved component. **Global Change Biology**, John Wiley and Sons Inc, v. 28, p. 1458–1476, 4 Feb. 2022. ISSN 13652486. DOI: 10.1111/gcb.15999.

MARSHALL, B.; BISCOE, P. V. A Model for C<sub>3</sub> Leaves Describing the Dependence of Net Photosynthesis on Irradiance Downloaded from. **Journal of Experimental Botany**, v. 31, p. 29–39, 120 1980. Available from: <<http://jxb.oxfordjournals.org/>>.

MCCARTHY, H. R. et al. Canopy leaf area constrains [CO<sub>2</sub>]-induced enhancement of productivity and partitioning among aboveground carbon pools. **PNAS**, v. 103, 51 2006.

MEDLYN, B. E.; LOUSTAU, D.; DELZON, S. Temperature response of parameters of a biochemically based model of photosynthesis. I. Seasonal changes in mature maritime pine ( *Pinus pinaster* Ait.) **Plant, Cell and Environment**, v. 25, p. 1155–1165, 2002. DOI: 10.1046/j.0016-8025.2002.00890.x. Available from: <<https://onlinelibrary.wiley.com/doi/10.1046/j.1365-3040.2002.00890.x>>.

MEDLYN, B. E.; DUURSMA, R. A.; DE KAUWE, M. G., et al. The optimal stomatal response to atmospheric CO<sub>2</sub> concentration: Alternative solutions, alternative interpretations. **Agricultural and Forest Meteorology**, v. 182-183, p. 200–203, Dec. 2013. ISSN 01681923. DOI: 10.1016/j.agrformet.2013.04.019.

MEDLYN, B. E.; DUURSMA, R. A.; EAMUS, D., et al. Reconciling the optimal and empirical approaches to modelling stomatal conductance. **Global Change Biology**, v. 17, p. 2134–2144, 6 June 2011. ISSN 13541013. DOI: 10.1111/j.1365-2486.2010.02375.x.

MENEZES, J. et al. Changes in leaf functional traits with leaf age: when do leaves decrease their photosynthetic capacity in Amazonian trees? **Tree Physiology**, v. 42, p. 922–938, 5 2022. DOI: 10.1093/treephys/tpab042.

MORISON, J. I. L. Stomatal response to increased CO<sub>2</sub> concentration. **Journal of Experimental Botany**, v. 49, p. 443–452, 1998. Available from: <<https://www.jstor.org/stable/23695977>>.

NEWINGHAM, B. A. et al. Does a decade of elevated [CO<sub>2</sub>] affect a desert perennial plant community? **New Phytologist**, v. 201, p. 498–504, 2 Jan. 2014. ISSN 0028646X. DOI: 10.1111/nph.12546.

OLIVEIRA, E. A. D. D. et al. Soil-nutrient availability modifies the response of young pioneer and late successional trees to elevated carbon dioxide in a Brazilian tropical environment. **Environmental and Experimental Botany**, v. 77, p. 53–62, Apr. 2012. ISSN 00988472. DOI: 10.1016/j.envexpbot.2011.11.003.

OREN, R. et al. Estimating the uncertainty in annual net ecosystem carbon exchange: Spatial variation in turbulent fluxes and sampling errors in eddy-covariance measurements. **Global Change Biology**, v. 12, p. 883–896, 5 May 2006. ISSN 13541013. DOI: 10.1111/j.1365-2486.2006.01131.x.

OTTOSEN, C. O.; MORTENSEN, L. M.; GISLERØD, H. R. Effect of Relative Air Humidity on Gas Exchange, Stomatal Conductance and Nutrient Uptake in Miniature Potted Roses. **Gartenbauwissenschaft**, v. 67, p. 143–147, 4 2002.

PEREIRA, I. S. et al. Performance of laser-based electronic devices for structural analysis of Amazonian terra-firme forests. **Remote Sensing**, MDPI AG, v. 11, 5 Mar. 2019. ISSN 20724292. DOI: 10.3390/rs11050510.

RAE, J. W. B. et al. Atmospheric CO<sub>2</sub> over the Past 66 Million Years from Marine Archives. **The Annual Review of Earth and Planetary Sciences is online at earth.annualreviews.org**, v. 49, p. 609–650, 2021. DOI:

10.1146/annurev-earth-082420. Available from:

<<https://doi.org/10.1146/annurev-earth-082420->>.

SOUZA, G. M. et al. Photosynthetic responses of four tropical tree species grown under gap and understorey conditions in a semi-deciduous forest. **Brazilian Journal of Botany**, v. 33, p. 529–538, 2010.

STINZIANO, J. et al. **photosynthesis: Tools for Plant Ecophysiology & Modeling**. 2023. Available from:

<<https://CRAN.R-project.org/package=photosynthesis>>. Visited on: 10 June 2024.

TANAKA, L. M.; SATYAMURTY, P.; MACHADO, L. A. Diurnal variation of precipitation in central Amazon Basin. **International Journal of Climatology**, John Wiley and Sons Ltd, v. 34, p. 3574–3584, 13 Nov. 2014. ISSN 10970088. DOI: 10.1002/joc.3929.

THOMAS, R. B.; DELUCIA, E. H. Photosynthetic responses to CO<sub>2</sub> enrichment of four hardwood species in a forest understory. **Oecologia**, v. 122, p. 11–19, 2000. DOI: 10.1007/PL00008827.

TURNER, B. L.; BRENES-ARGUEDAS, T.; CONDIT, R. Pervasive phosphorus limitation of tree species but not communities in tropical forests. **Nature**, Nature Publishing Group, v. 555, p. 367–370, 7696 Mar. 2018. ISSN 14764687. DOI: 10.1038/nature25789.

WANG, D. et al. A meta-analysis of plant physiological and growth responses to temperature and elevated CO<sub>2</sub>. **Oecologia**, v. 169, p. 1–13, 1 May 2012. ISSN 00298549. DOI: 10.1007/s00442-011-2172-0.

WÜRTH, M. K.; WINTER, K.; KÖRNER, C. In situ responses to elevated CO<sub>2</sub> in tropical forest understorey plants. **Functional Ecology**, v. 12, p. 886–895, 6 1998. ISSN 02698463. DOI: 10.1046/j.1365-2435.1998.00278.x.

XU, Z.; JIANG, Y.; JIA, B., et al. Elevated-CO<sub>2</sub> response of stomata and its dependence on environmental factors. **Frontiers in Plant Science**, Frontiers Media S.A., v. 7, MAY2016 May 2016. ISSN 1664462X. DOI: 10.3389/fpls.2016.00657.

XU, Z.; JIANG, Y.; ZHOU, G. Response and adaptation of photosynthesis, respiration, and antioxidant systems to elevated CO<sub>2</sub> with environmental stress in plants. **Frontiers in Plant Science**, Frontiers Media S.A., v. 6, September Sept. 2015. ISSN 1664462X. DOI: 10.3389/fpls.2015.00701.

YU, K. C.; RAYNOLDS, R. **Climate Change for Astronomers: causes, consequences, and communication**. [S.l.]: IOP Publishing Ltd, 2024. chap. 2. ISBN 978-0-7503-3727-4.

ZEIGER, E.; FARQUHAR, G.; COWAN, I. **Stomatal Function**. [S.l.]: Stanford University Press, 1987. ISBN 9780804713474. Available from: <https://books.google.com.br/books?id=mp-aAAAAIAAJ>.

ZELIKOVA, T. J. et al. Long-term exposure to elevated CO<sub>2</sub> enhances plant community stability by suppressing dominant plant species in a mixed-grass prairie. **Proceedings of the National Academy of Sciences of the United States of America**, National Academy of Sciences, v. 111, p. 15456–15461, 43 Oct. 2014. ISSN 10916490. DOI: 10.1073/pnas.1414659111.

ZHAN, C. et al. Emergence of the physiological effects of elevated CO<sub>2</sub> on land–atmosphere exchange of carbon and water. **Global Change Biology**, John Wiley and Sons Inc, v. 28, p. 7313–7326, 24 Dec. 2022. ISSN 13652486. DOI: 10.1111/gcb.16397.

# Appendix

Presented in this appendix are additional figures that detail parts of the results and methodology described in the past sections. All code and data produced in this study are available at <https://doi.org/10.25824/redu/C3H4KW>.

## A.1 Additional tables

**Table A.1:** Confounding factors significance - Model formulas and p-value results for species, experimental groups, relative growth rate (*rg*) and soil water content (*wsoil*).

| Formula   | First p-value           | Second p-value       |
|---|-------------------------|----------------------|
| $g1 \sim \text{species} + \text{wsoil}$                 | $8.69 \cdot 10^{-1}$    | $4.24 \cdot 10^{-1}$ |
| $g1 \sim \text{experiment} + \text{wsoil}$              | $2.68 \cdot 10^{-1}$    | $6.35 \cdot 10^{-1}$ |
| $g1 \sim \text{species} + \text{rg}$                    | $8.32 \cdot 10^{-1}$    | $1.22 \cdot 10^{-1}$ |
| $g1 \sim \text{experiment} + \text{rg}$                 | $3.84 \cdot 10^{-1}$    | $1.23 \cdot 10^{-1}$ |
| $gk \sim \text{species} + \text{wsoil}$                 | $4.07 \cdot 10^{-1}$    | $9.53 \cdot 10^{-1}$ |
| $gk \sim \text{experiment} + \text{wsoil}$              | $8.97 \cdot 10^{-1}$    | $9.44 \cdot 10^{-1}$ |
| $gk \sim \text{species} + \text{rg}$                    | $7.61 \cdot 10^{-1}$    | $9.62 \cdot 10^{-1}$ |
| $gk \sim \text{experiment} + \text{rg}$                 | $7.53 \cdot 10^{-1}$    | $7.28 \cdot 10^{-1}$ |
| $gs \sim \text{species} + \text{wsoil}$                 | $1.31 \cdot 10^{-2} *$  | $6.90 \cdot 10^{-1}$ |
| $gs \sim \text{experiment} + \text{wsoil}$              | $1.10 \cdot 10^{-1}$    | $3.33 \cdot 10^{-1}$ |
| $gs \sim \text{species} + \text{rg}$                    | $7.10 \cdot 10^{-5} *$  | $9.35 \cdot 10^{-1}$ |
| $gs \sim \text{experiment} + \text{rg}$                 | $9.35 \cdot 10^{-1}$    | $6.02 \cdot 10^{-1}$ |
| $E \sim \text{species} + \text{wsoil}$                  | $2.05 \cdot 10^{-10} *$ | $4.74 \cdot 10^{-1}$ |
| $E \sim \text{experiment} + \text{wsoil}$               | $1.30 \cdot 10^{-1}$    | $6.32 \cdot 10^{-1}$ |
| $E \sim \text{species} + \text{rg}$                     | $1.27 \cdot 10^{-8} *$  | $8.74 \cdot 10^{-1}$ |
| $E \sim \text{experiment} + \text{rg}$                  | $2.10 \cdot 10^{-1}$    | $3.24 \cdot 10^{-1}$ |
| $V_{\text{cmax}} \sim \text{species} + \text{wsoil}$    | $7.15 \cdot 10^{-1}$    | $1.47 \cdot 10^{-1}$ |
| $V_{\text{cmax}} \sim \text{experiment} + \text{wsoil}$ | $7.17 \cdot 10^{-1}$    | $1.85 \cdot 10^{-1}$ |
| $V_{\text{cmax}} \sim \text{species} + \text{rg}$       | $8.54 \cdot 10^{-1}$    | $3.34 \cdot 10^{-1}$ |
| $V_{\text{cmax}} \sim \text{experiment} + \text{rg}$    | $6.60 \cdot 10^{-1}$    | $1.90 \cdot 10^{-1}$ |
| $J_{\text{max}} \sim \text{species} + \text{wsoil}$     | $6.98 \cdot 10^{-1}$    | $5.10 \cdot 10^{-1}$ |
| $J_{\text{max}} \sim \text{experiment} + \text{wsoil}$  | $6.87 \cdot 10^{-1}$    | $3.19 \cdot 10^{-1}$ |
| $J_{\text{max}} \sim \text{species} + \text{rg}$        | $6.58 \cdot 10^{-1}$    | $7.62 \cdot 10^{-1}$ |
| $J_{\text{max}} \sim \text{experiment} + \text{rg}$     | $6.54 \cdot 10^{-1}$    | $9.60 \cdot 10^{-1}$ |

**Table A.2:** Leaf area (in square meters) for experimental groups and species is presented alongside the total leaf area of all individuals within the OTCs. Data from outside control groups is not shown.

| Leaf area ( $m^2$ ) | <i>D. flagellaris</i> | <i>P. grandiflora</i> | Both combined | All species |
|---------------------|-----------------------|-----------------------|---------------|-------------|
| Control             | 0.0636                | 0.0470                | 0.1106        | 0.4480      |
| Treatment           | 0.0197                | 0.1464                | 0.1661        | 0.4998      |
| Total               | 0.0833                | 0.1935                | 0.2767        | 0.9478      |

## A.2 Stomatal conductance measurements from A/Ci and A/Q curves

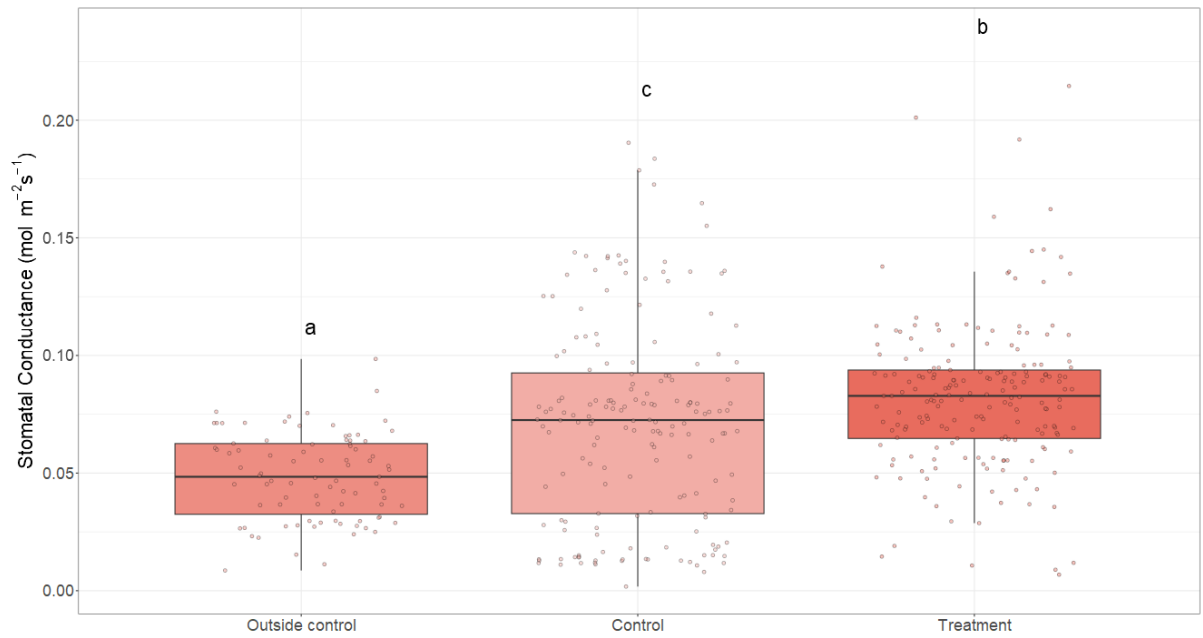


**Figure A.1:** Stomatal conductance values measured during A/Ci response curves separated by experimental groups. The Tukey test shows that each boxplot is significantly different from each other.

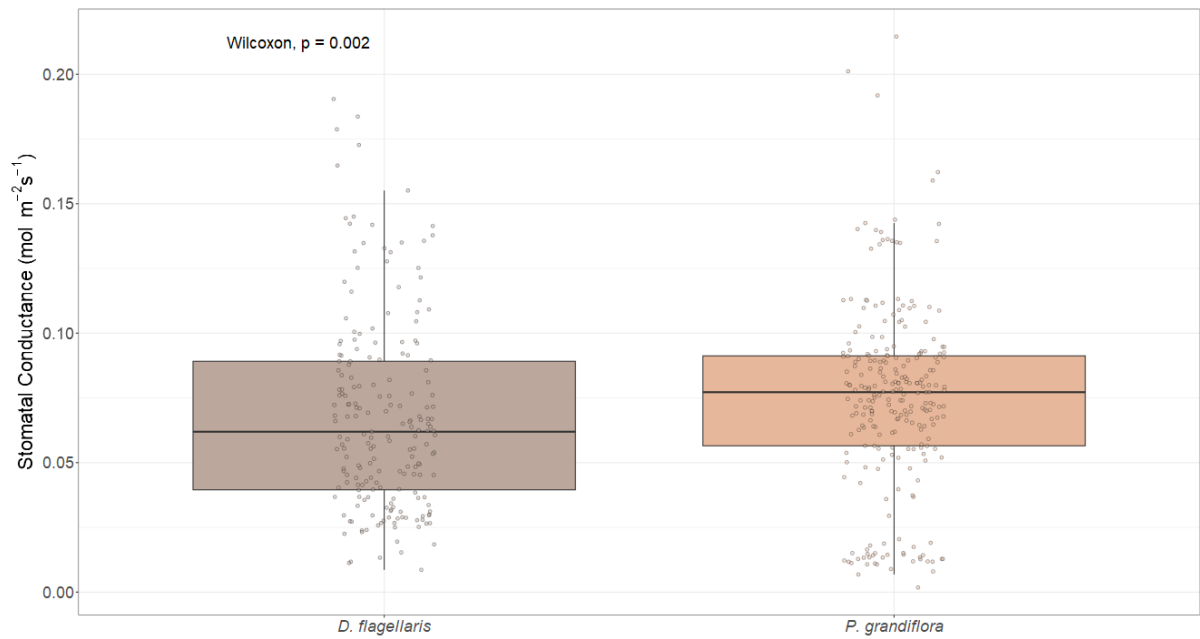


**Figure A.2:** Stomatal conductance values measured during A/Ci response curves separated by species. The Wilcoxon test p-value shows a significant difference between the species.

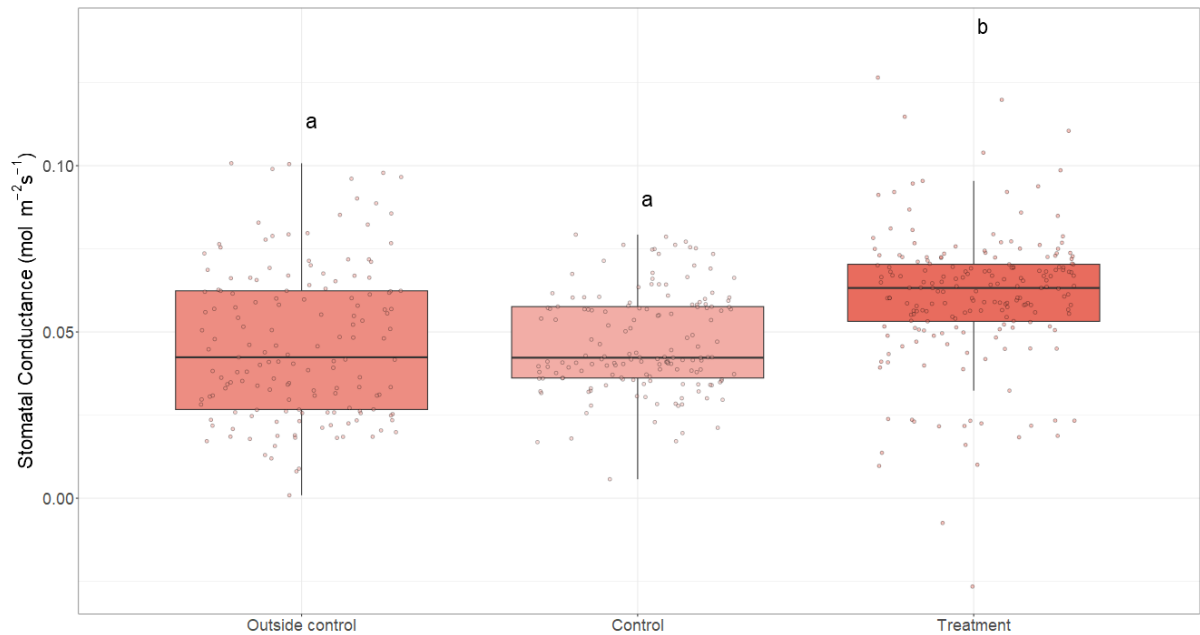


**Figure A.3:** Stomatal conductance values measured during A/Q response curves separated by experimental groups. The Tukey test shows that the treatment boxplot is significantly different from the others.

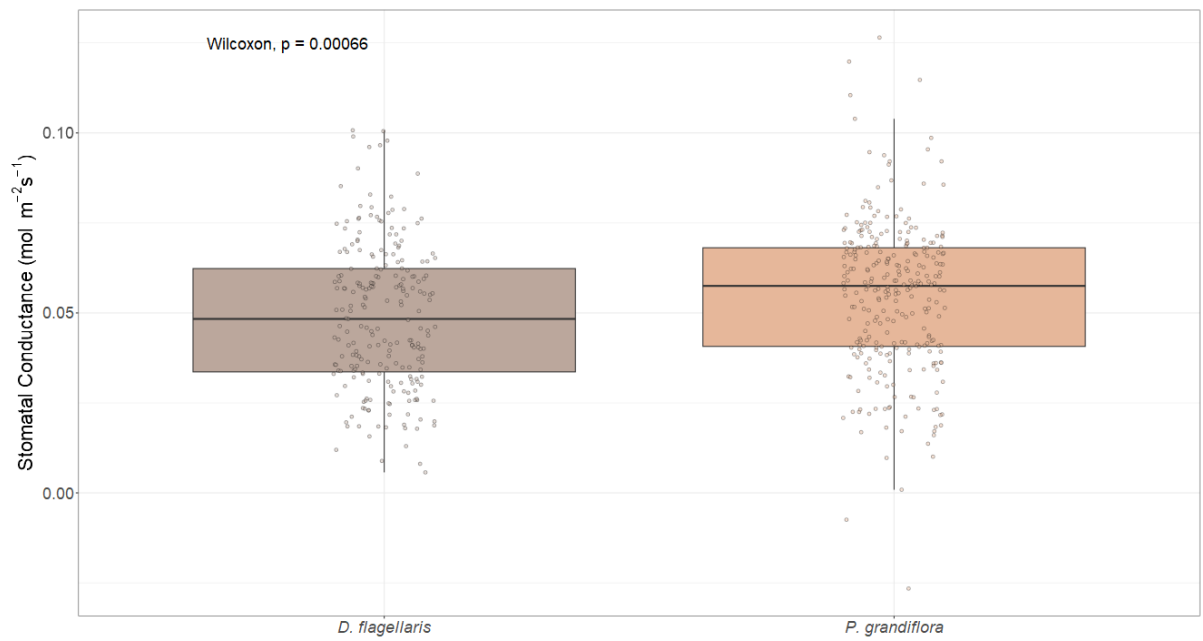


**Figure A.4:** Stomatal conductance values measured during A/Q response curves separated by species. The Wilcoxon test p-value shows a significant difference between the species.

### A.3 $J_{max} / V_{cmax}$ ratio plots

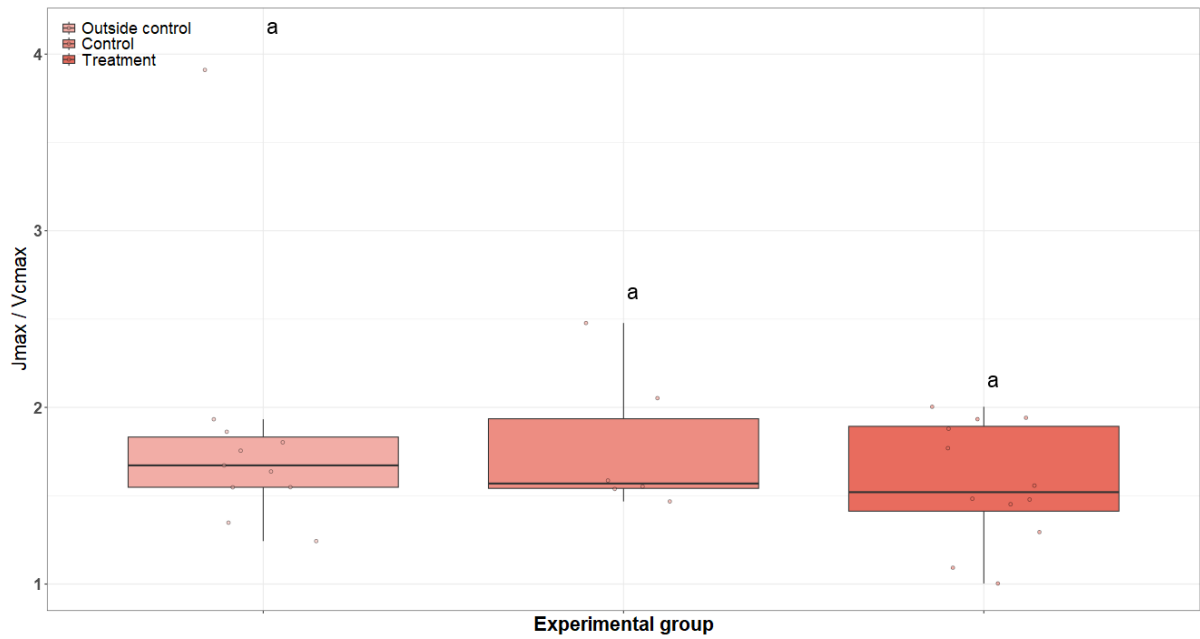


**Figure A.5:** Ratio of the values of  $J_{max}$  and  $V_{cmax}$  separated by experimental group. The Tukey test shows no significant changes between groups.

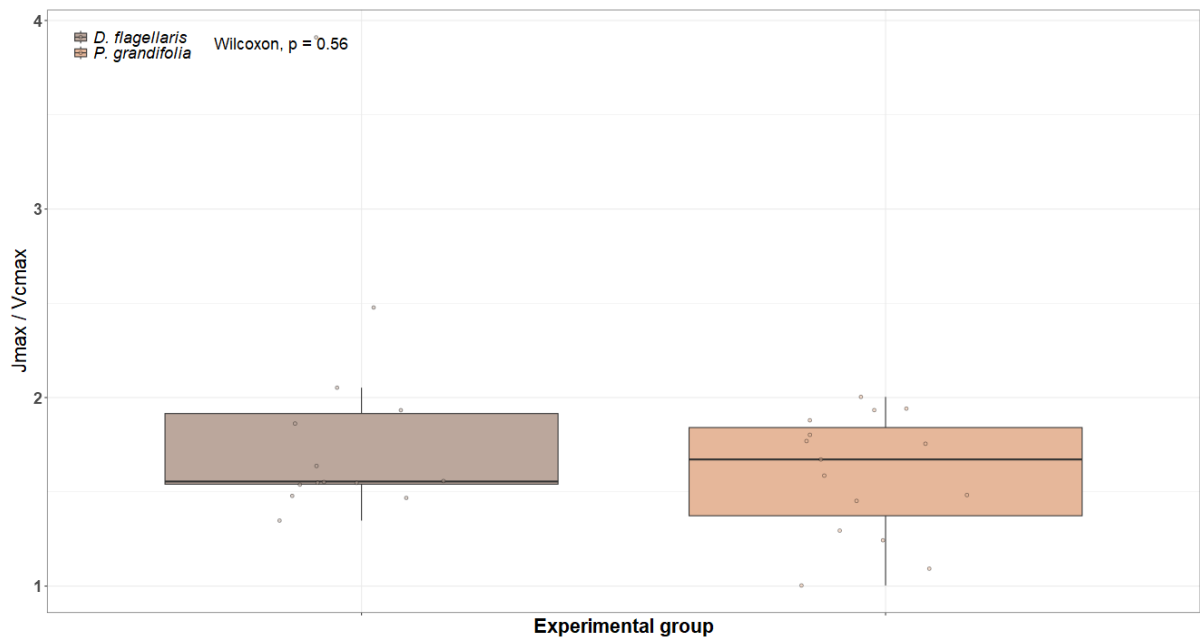


**Figure A.6:** Ratio of the values of  $J_{max}$  and  $V_{cmax}$  separated by species. The Wilcoxon p-value shows no significant changes between species.

### A.4 Examples of response curves measured at the experimental site

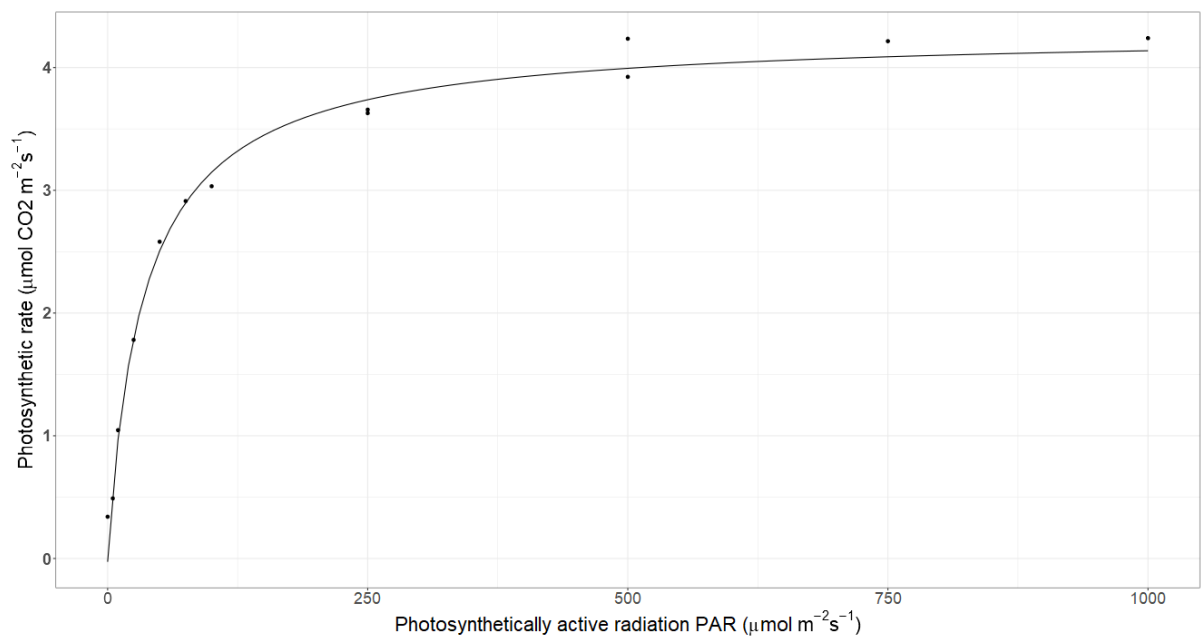


Figure A.7: Example of A/Q response curve of the individual 101.

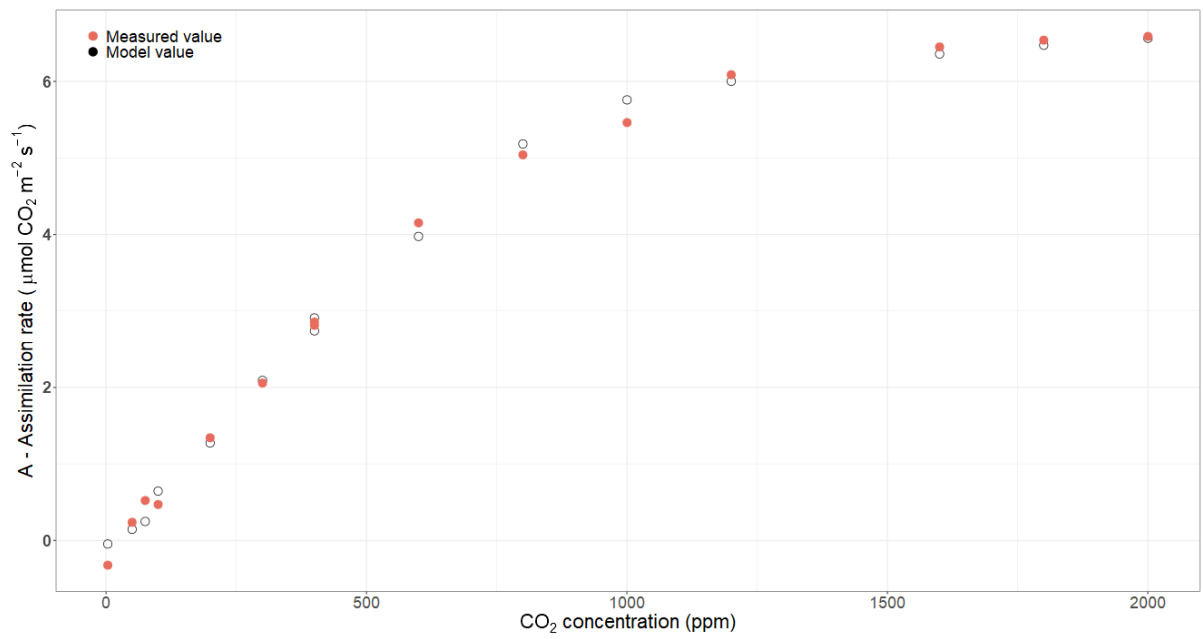
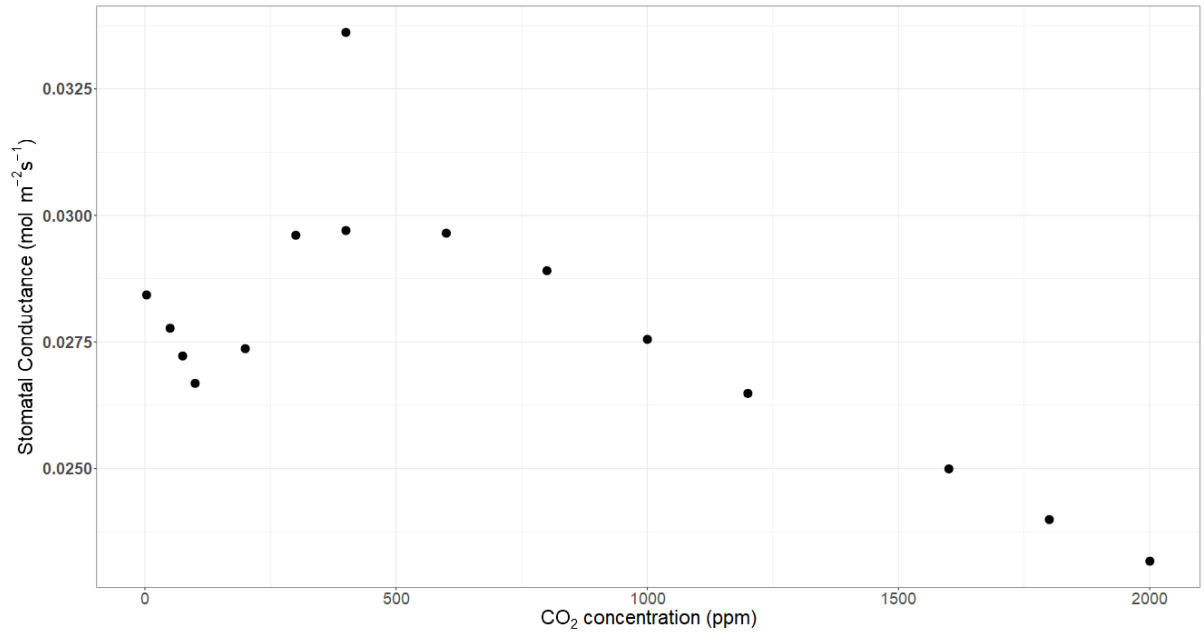
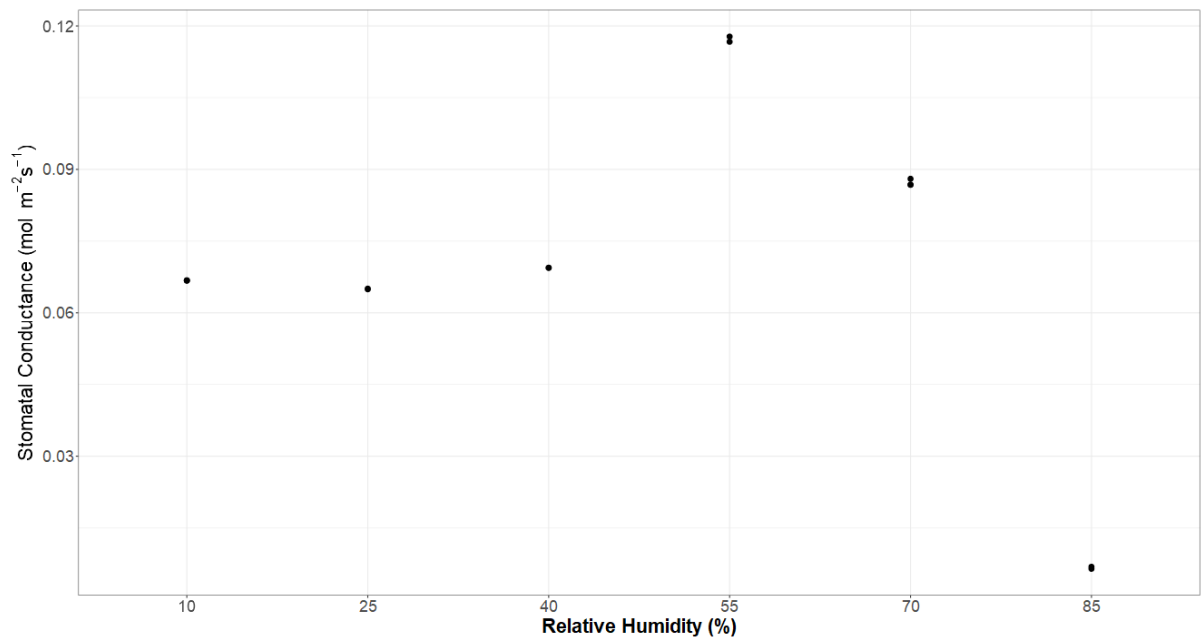


Figure A.8: Example of A/Ci response curve of the individual 604.



**Figure A.9:** Example of stomatal conductance response to the increase of CO<sub>2</sub>, for the individual 604.



**Figure A.10:** Example of A/RH response curve of the individual 101.

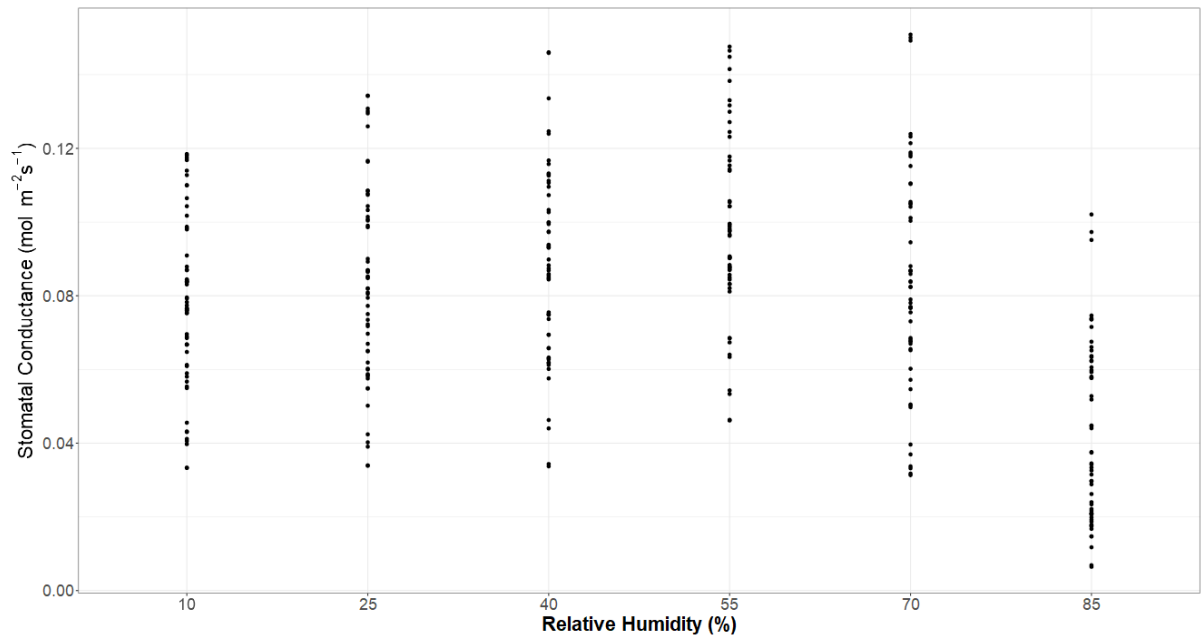


**Figure A.11:** A/RH response curve combined values rounded in the x axis to the RH intervals

## A.5 Individual leaf area

The leaf area measurements for each individual from the two species analysed in the present study can be found are shown in the following plots, which demonstrate the differences between experimental groups and species.

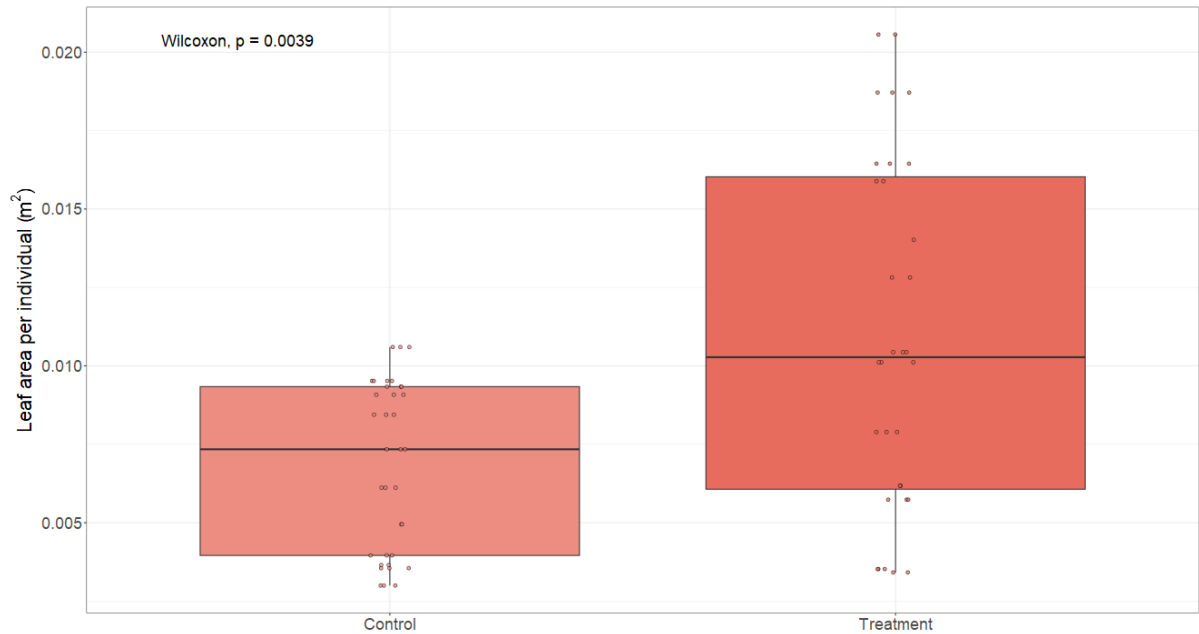


**Figure A.12:** Boxplots showing the leaf area values measured in the field, separated between control and treatment individuals. The leaf area found for the treatment group is significantly higher.

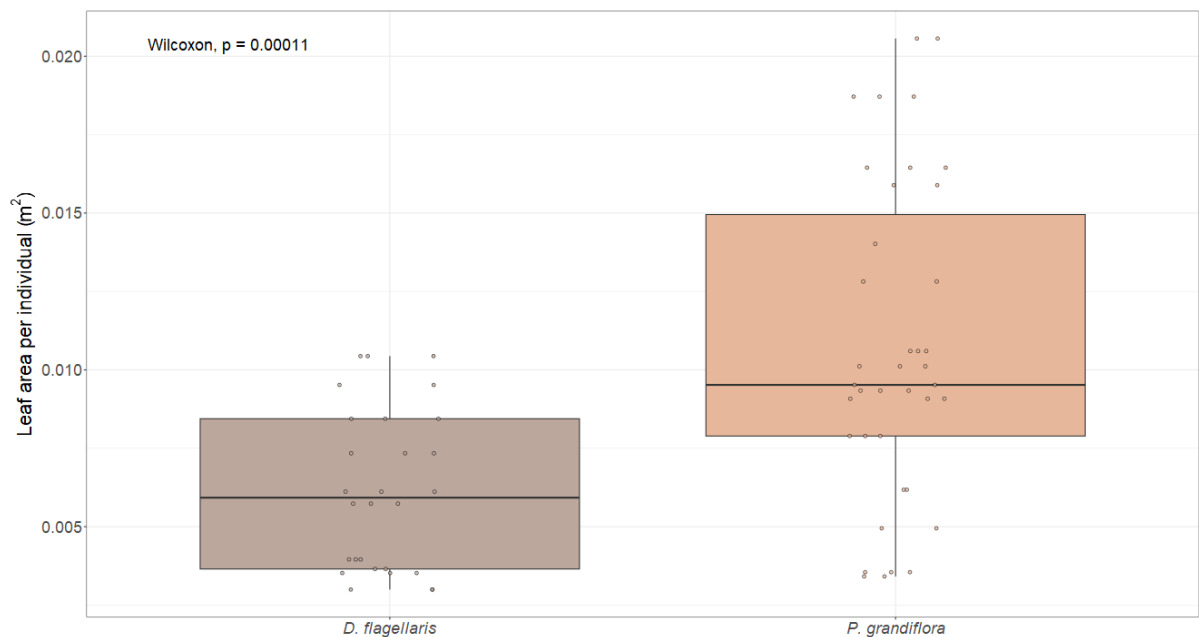


**Figure A.13:** Boxplots showing the leaf area values measured in the field, separated between species. The leaf area found for *P. grandiflora* is significantly higher.

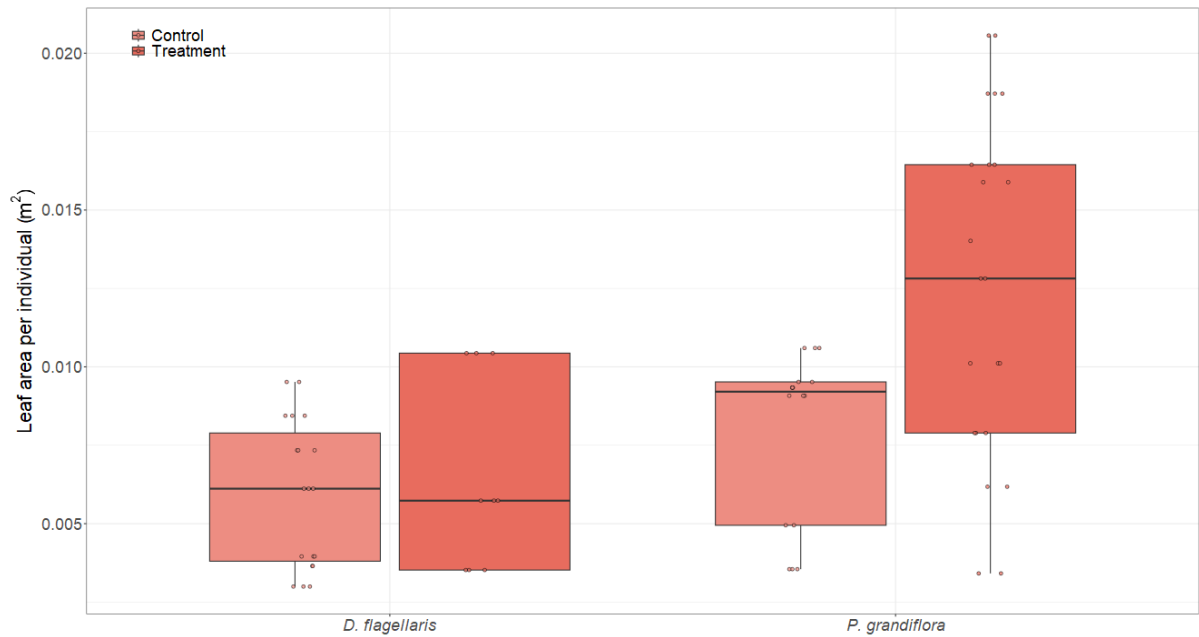


**Figure A.14:** Boxplots showing the leaf area values measured in the field, separated between species and experimental groups. The results show that most of the difference observed between experimental groups is caused by *P. grandiflora*, while *D. flagellaris* values are much more similar.

## A.6 Big leaf upscaling: additional plots

As mentioned in the methodology, the upscaling was conducted with varying gk parameters and fixed gk. Since the final boxplots are rather similar, the estimates with fixed gk and the plots for net CO<sub>2</sub> assimilation and stomatal conductance are presented below.

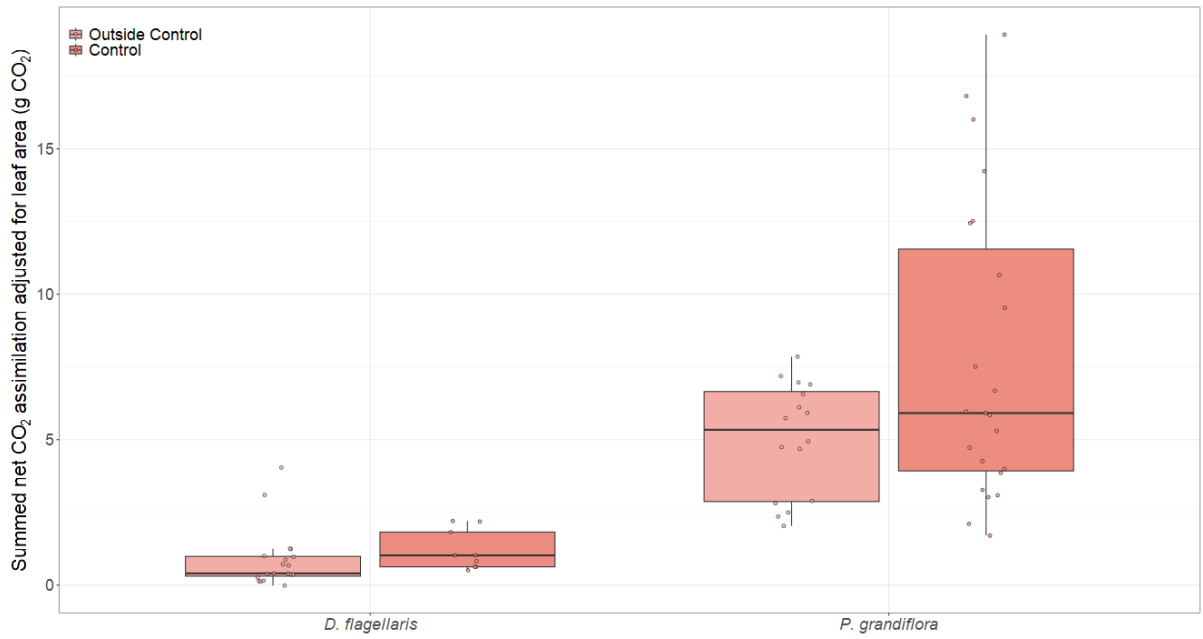


**Figure A.15:** Boxplots showing the net CO<sub>2</sub> assimilation values separated by species and experimental groups. The boxplots show a slight increase of values in the treatment group for both species.

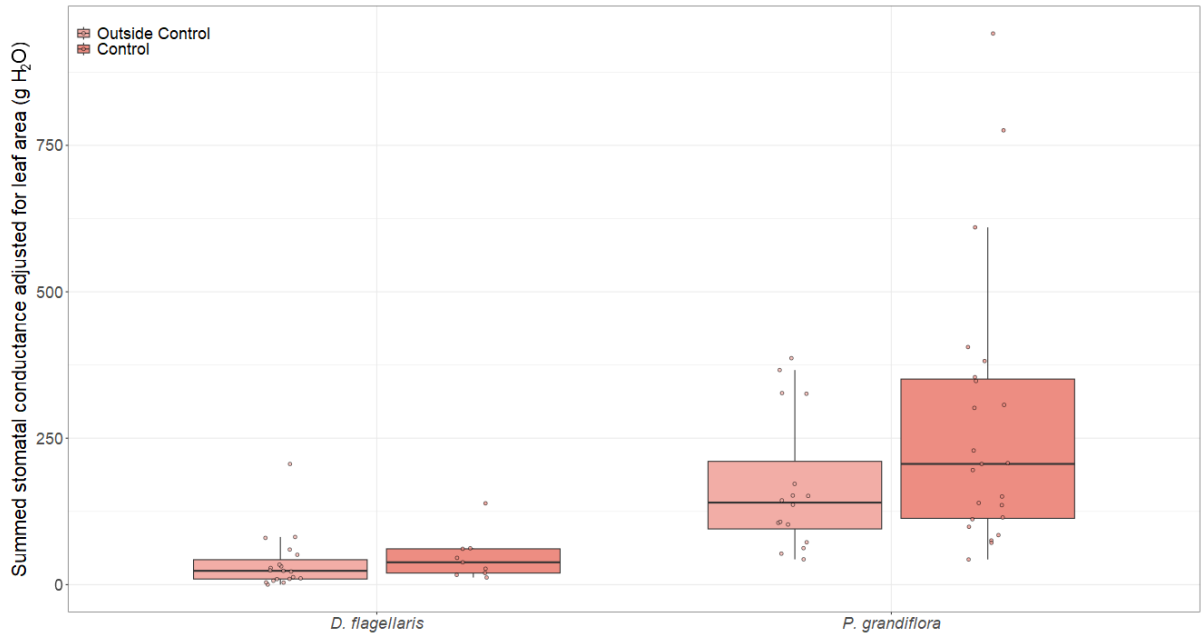


**Figure A.16:** Boxplots showing the stomatal conductance values estimated by the big leaf model separated by species and experimental groups. The boxplots show a slight increase of values in the treatment group for both species, with much higher values for *P. grandiflora*.

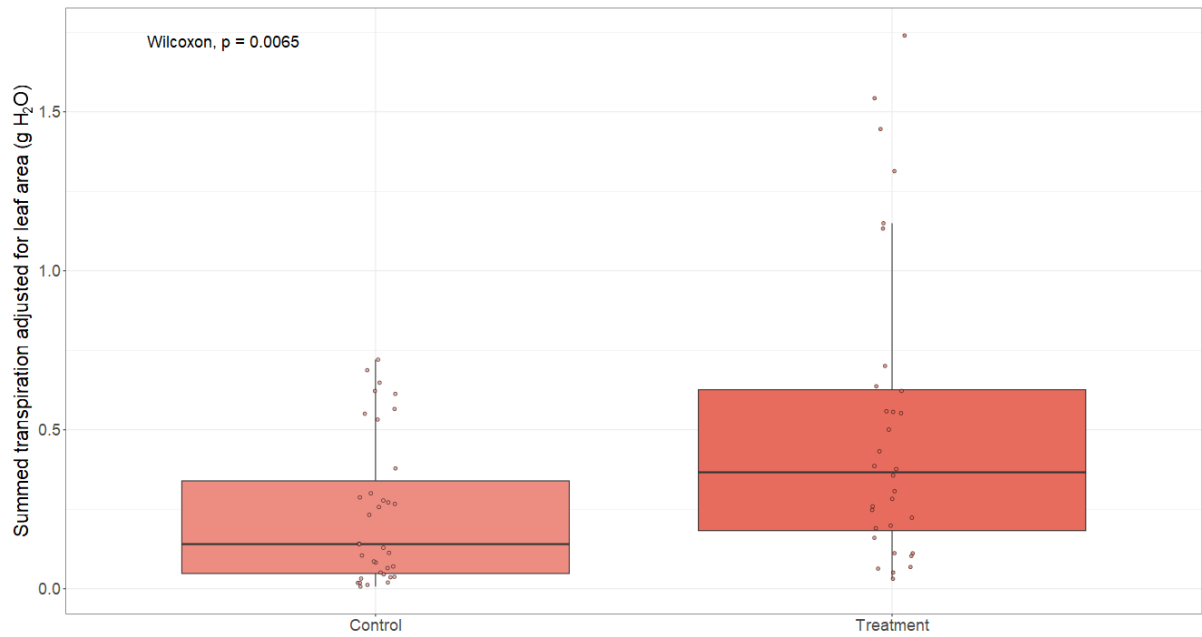


**Figure A.17:** Boxplots showing the transpiration values estimated by the big leaf model using the partial Medlyn (fixed  $g_k$ ) model parameters separated by experimental group. The Tukey test indicates a significant increase in the treatment group in relation to the other two.

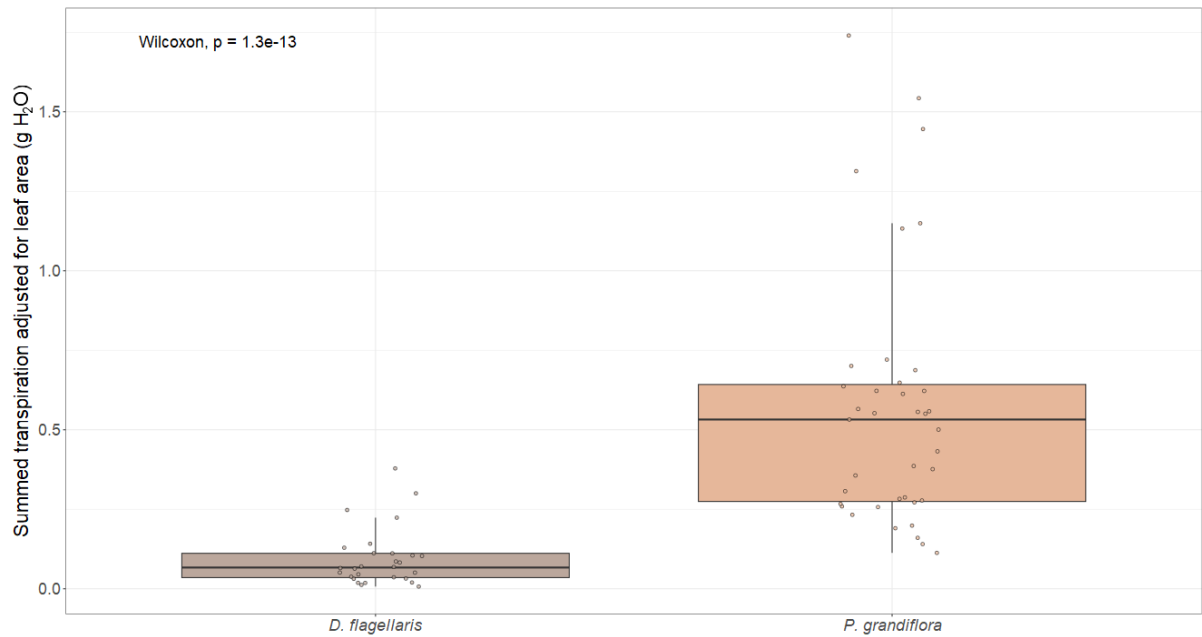


**Figure A.18:** Boxplots showing the transpiration values estimated by the big leaf model using the partial Medlyn (fixed  $g_k$ ) model parameters separated by species. The Wilcoxon p-value indicates a significant difference between the two boxplots.

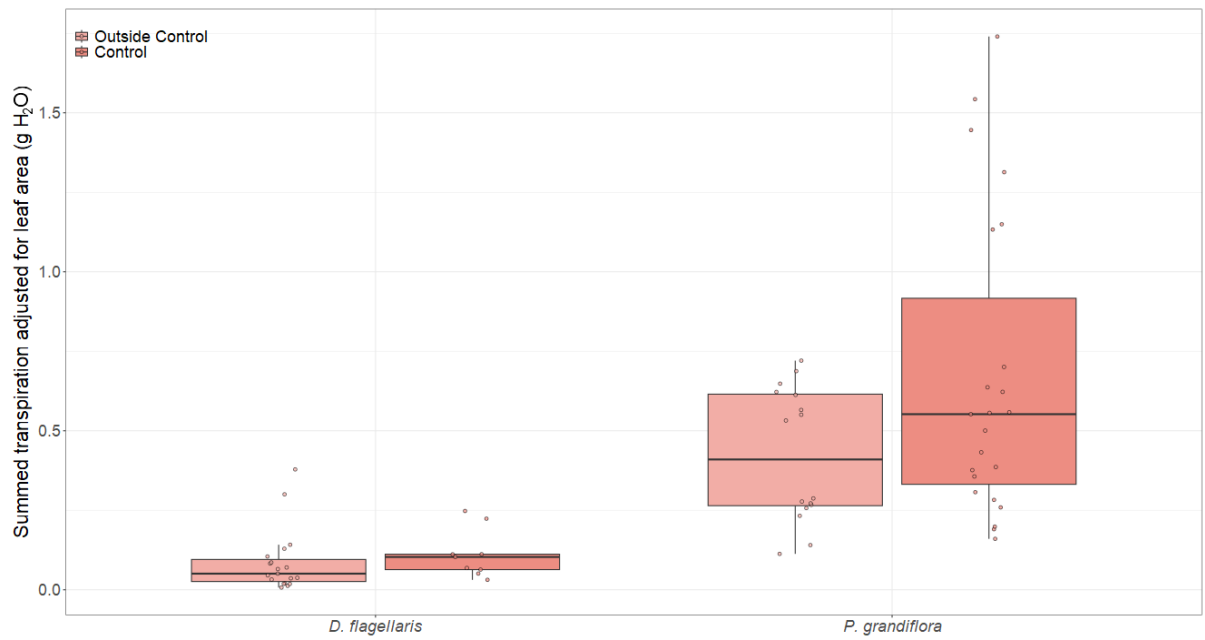


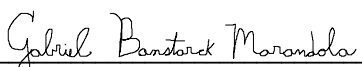
**Figure A.19:** Boxplots showing the transpiration values estimated by the big leaf model using the partial Medlyn (fixed  $g_k$ ) model parameters separated by species and experimental groups. The boxplots show no consistent differences in experimental groups present for both species.


## A.7 Declaration of copyright

### Declaração

As cópias de artigos de minha autoria ou de minha co-autoria, já publicados ou submetidos para publicação em revistas científicas ou anais de congressos sujeitos a arbitragem, que constam da minha Dissertação/Tese de Mestrado/Doutorado, intitulada **Evaluation of CO<sub>2</sub> rising effects on understory vegetation transpiration in Central Amazonia through an experiment-modeling integrated approach (Avaliação dos efeitos do CO<sub>2</sub> elevado sobre a transpiração da vegetação de sub-bosque na Amazônia Central através de integração experimento-modelagem)**, não infringem os dispositivos da Lei n.º 9.610/98, nem o direito autoral de qualquer editora.

Campinas, 24 de outubro de 2024

Assinatura :   
Nome do autor: **Gabriel Banstarck Marandola**  
RG n.º 49.833.221-4

Assinatura :   
Nome do(a) orientador(a): **David Montenegro Lapola**  
RG n.º 30.568.373-1

## A.8 Declaration of bioethics and biosafety



COORDENADORIA DE PÓS-GRADUAÇÃO  
INSTITUTO DE BIOLOGIA  
Universidade Estadual de Campinas  
Caixa Postal 6109. 13083-970, Campinas, SP, Brasil  
Fone (19) 3521-6378. email: cpgib@unicamp.br



### DECLARAÇÃO

Em observância ao **§5º do Artigo 1º da Informação CCPG-UNICAMP/001/15**, referente a Bioética e Biossegurança, declaro que o conteúdo de minha dissertação de mestrado, intitulada **Evaluation of CO<sub>2</sub> rising effects on understory vegetation transpiration in Central Amazonia through an experiment-modeling integrated approach (Avaliação dos efeitos do CO<sub>2</sub> elevado sobre a transpiração da vegetação de sub-bosque na Amazônia Central através de integração experimento-modelagem)**, desenvolvida no Programa de Pós-Graduação em Ecologia do Instituto de Biologia da Unicamp, não versa sobre pesquisa envolvendo seres humanos, animais ou temas afetos à Biossegurança.

Assinatura: Gabriel Banstarck Marandola  
Nome do aluno: Gabriel Banstarck Marandola

Assinatura: David Montenegro Lapola  
Nome do orientador: David Montenegro Lapola

Data: 25/10/2024